PALEOCEANOGRAPHY, VOL. 25, PA1206, doi:10.1029/2008PA001671, 2010

Last Glacial Maximum to Holocene sea surface conditions at Umnak Plateau, Bering Sea, as inferred from diatom, alkenone, and stable isotope records

Beth E. Caissie,[1] Julie Brigham-Grette,[1] Kira T. Lawrence,[2] Timothy D. Herbert,[3] and Mea S. Cook[4]

Received 5 August 2008; revised 15 September 2009; accepted 30 September 2009; published 9 February 2010.

[1] The Bering Sea gateway between the Pacific and Arctic oceans impacts global climate when glacial-interglacial shifts in shore line position and ice coverage change regional albedo. Previous work has shown that during the last glacial termination and into the Holocene, sea level rises and sea ice coverage diminishes from perennial to absent. Yet, existing work has not quantified sea ice duration or sea surface temperatures (SST) during this transition. Here we combine diatom assemblages with the first alkenone record from the Bering Sea to provide a semiquantitative record of sea ice duration, SST, and productivity change since the Last Glacial Maximum (LGM). During the LGM, diatom assemblages indicate that sea ice covered the southeastern Bering Sea perennially. At 15.1 cal ka B.P., the diatom assemblage shifts to one more characteristic of seasonal sea ice and alkenones occur in the sediments in low concentrations. Deglaciation is characterized by laminated intervals with highly productive and diverse diatom assemblages and inferred high coccolithophorid production. At 11.3 cal ka B.P. the diatom assemblage shifts from one dominated by sea ice species to one dominated by a warmer water, North Pacific species. Simultaneously, the SST increases by 3°C and the southeastern Bering Sea becomes ice-free year-round. Productivity and temperature proxies are positively correlated with independently dated records from elsewhere in the Bering Sea, the Sea of Okhotsk, and the North Pacific, indicating that productivity and SST changes are coeval across the region.

Citation: Caissie, B. E., J. Brigham-Grette, K. T. Lawrence, T. D. Herbert, and M. S. Cook (2010), Last Glacial Maximum to Holocene sea surface conditions at Umnak Plateau, Bering Sea, as inferred from diatom, alkenone, and stable isotope records, *Paleoceanography*, *25*, PA1206, doi:10.1029/2008PA001671.

1. Introduction

[2] The Arctic region has registered the greatest impacts of climate change over the past 100 years largely due to the ice-albedo feedback [*Intergovernmental Panel on Climate Change*, 2007]. Sea ice is a defining characteristic of the Arctic Ocean, yet sea ice extent has been rapidly declining since 1979 [*Serreze et al.*, 2007] with record lows in 2005 and 2007 [*Stroeve et al.*, 2008]. Sea ice also controls the timing and location of the extremely productive spring phytoplankton bloom [*Stabeno et al.*, 2001] which prompts enough organic matter to settle to the seafloor and sustain the entire shelf ecosystem throughout the year [*Walsh and McRoy*, 1986; *Stockwell et al.*, 2001; *Lovvorn et al.*, 2005]. Climate models predict that as Arctic temperatures continue to warm, summer sea ice will disappear from the Arctic Ocean, potentially as early as 2037 [*Holland et al.*, 2006; *Wang and Overland*, 2009]. By 2100, the maximum extent of winter sea ice in the Bering Sea could be more than 500 km north of its limit today [*Arzel et al.*, 2006] (Figure 1 and Table 1).

[3] Extensive international programs have been launched to monitor northern hemisphere sea ice changes and to develop models for predicting the magnitude and direction of Arctic environmental change into the future [e.g., *Study of Environmental Arctic Change*, 2005; *International Study of Arctic Change*, 2009; DAMOCLES, Developing Arctic Modeling and Observing Capabilities for Long-term Environmental Studies, 2007, available at http://www.damocles-eu.org/index.shtml]. High-resolution paleoclimate records can help inform efforts to model rapid contemporary changes by providing insight into Arctic system dynamics and environmental thresholds. Data sets of past temperatures and sea ice extent provide accurate boundary conditions for testing and validating model outputs. The sea surface temperature (SST) and sea ice components within many general circulation models are still often tuned to *CLIMAP Project Members* [1981] [e.g., *Hewitt et al.*, 2001], and although some sea ice models have been tested against paleodata, most of these focus only on the North Atlantic and Antarctica [e.g., *Hewitt*

[1]Department of Geosciences, University of Massachusetts Amherst, Amherst, Massachusetts, USA.
[2]Department of Geology and Environmental Geosciences, Lafayette College, Easton, Pennsylvania, USA.
[3]Department of Geological Sciences, Brown University, Providence, Rhode Island, USA.
[4]Geosciences Department, Williams College, Williamstown, Massachusetts, USA.

0883-8305/10/2008PA001671$12.00

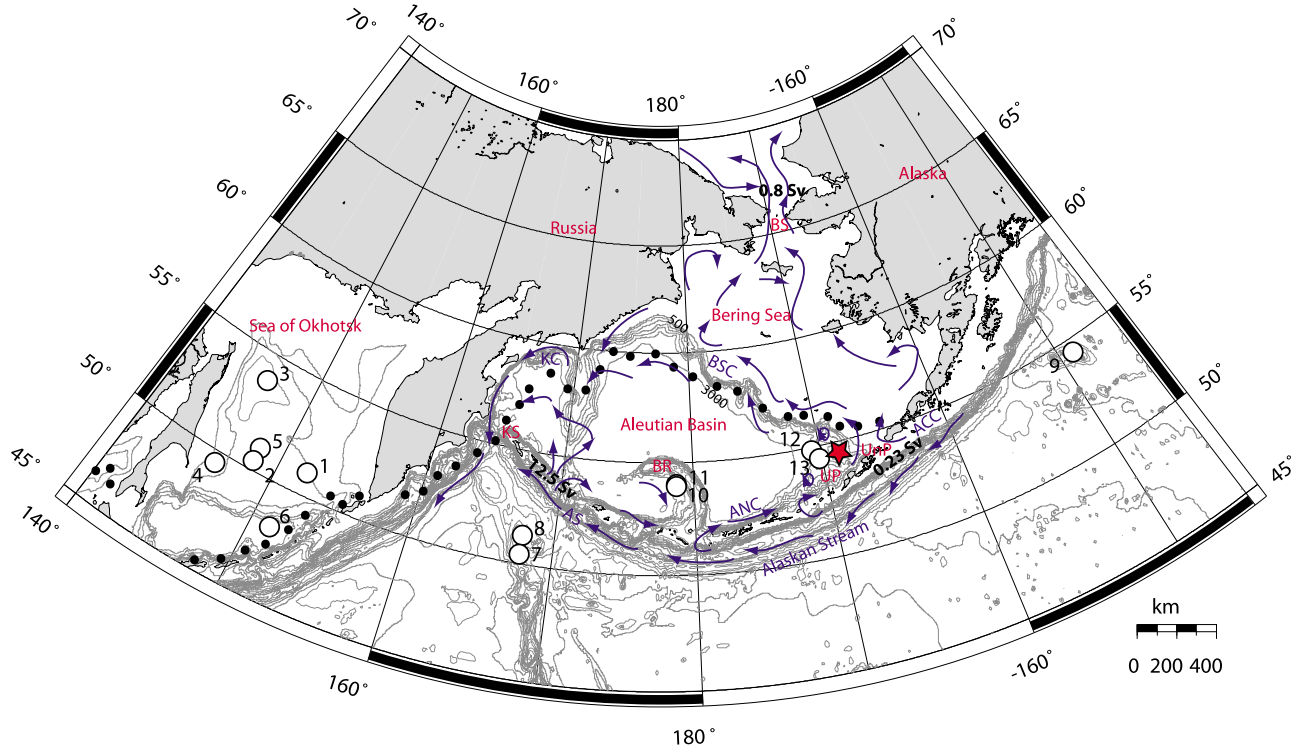

Figure 1. Map of the North Pacific, Bering Sea, and Sea of Okhotsk with locations of cores mentioned in the text. White circles denote cores described in previous studies (see Table 1 for core names and references); the red star denotes the location of 51JPC. Generalized ocean circulation is included for the Bering Sea (modified from *Stabeno et al.* [1999, 2001]), and maximum sea ice extent for the years 1979–2007 lies north of the black dotted line [*Stroeve and Meier*, 1999]. The Umnak Plateau (UP), Bowers Ridge (BR), Unimak Pass (UnP), Bering Strait (BS), and Kamchatka Strait (KS) are labeled in red; the Kamchatka Current (KC), Alaskan Stream (AS), Alaska Coastal Current (ACC), Aleutian North Slope Current (ANC), and Bering Slope Current (BSC) are labeled in dark blue. Contour interval is 500 m. Map created using Online Map Creation (http://www.aquarius.geomar.de/omc/).

et al., 2001, 2003; *Masson-Delmotte et al.*, 2006; *Kim et al.*, 2008]. This regional focus is partly due to a paucity of paleodata from the North Pacific. Here we provide a new sea ice and SST reconstruction from the Bering Sea, which places new constraints on the environmental history of the region.

[4] The Bering Sea lies in the far North Pacific between Alaska and Russia and serves as a transition between the

Table 1. Cores Referred to in the Text

Core[a]	Name	Source	General Area	Proxy
1	XP98-PC1	*Sakamoto et al.* [2005]	Sea of Okhotsk	IRD–Okhotsk sea ice expansion events
2	XP98-PC2	*Sakamoto et al.* [2005]	Sea of Okhotsk	IRD–Okhotsk sea ice expansion events
3	XP98-PC3	*Sakamoto et al.* [2005]	Sea of Okhotsk	IRD–Okhotsk sea ice expansion events
4	XP98-PC4	*Sakamoto et al.* [2005]	Sea of Okhotsk	IRD–Okhotsk sea ice expansion events
5	GC 936	*Gorbarenko et al.* [2004]	Sea of Okhotsk	$CaCO_3$ weight percent, $\delta^{18}O$
6	Nesmeyanov 25, GGC-15	*Keigwin* [1998]	Sea of Okhotsk	$\delta^{18}O$, C_{37} total, $U^{K'}_{37}$, phytol
7	Vinogradov 19/4, GGC-37	*Keigwin* [1998]	Detroit Seamount, N. Pacific	$\delta^{18}O$
8	MD01-2416	*Gebhardt et al.* [2008]	Detroit Seamount, N. Pacific	IRD, biogenic opal
9	MD02-2489	*Gebhardt et al.* [2008]	Patton Seamount, N. Pacific	$\delta^{18}O$, IRD, biogenic opal
10	HLY0202-17JPC	*Cook et al.* [2005]	Bowers Ridge, Bering Sea	$\delta^{18}O$
11	BOW 9A	*Katsuki and Takahashi* [2005] and *Okazaki et al.* [2005]	Bowers Ridge, Bering Sea	CaCO3 wt %
12	RC14-121	*Sancetta and Robinson* [1983]	Umnak Plateau, Bering Sea	diatom assemblages
13	UMK3A	*Katsuki and Takahashi* [2005] and *Okazaki et al.* [2005]	Umnak Plateau, Bering Sea	diatom assemblages, $CaCO_3$ weight %
Red star	HLY0202-51JPC	this study	Umnak Plateau, Bering Sea	diatom assemblages, $\delta^{13}C$, C_{37} total, $U^{K'}_{37}$, $\delta^{18}O$

[a]See core locations in Figure 1.

Table 2. Microorganisms Mentioned in the Text

Microorganism	Species
Foraminifera	
Benthic	*Elphidium excavatum* Terquem
Planktic	*Neogloboquadrina pachyderma* Ehrenberg (sinistral)
Coccolithophorid	*Emiliani huxleyi* Lohmann
Diatoms	
Centric	*Chaetoceros* Ehrenberg, *Coscinodiscus marginatus* Ehrenberg, *Odontella aurita* (Lyngbye) Agardh, *Rhizosolenia hebetata* forma *hiemalis* (Bailey) Gran, *Thalassiosira antarctica* var. *borealis* (Fryxell) Doucette and Hubbard resting spores, *Thalassiosira hyalina* (Grunow) Gran, *Thalassiosira nordenskioeldii* Cleve, *Thalassiosira trifulta* Fryxell[a]
Pennate	*Fragilariopsis cylindrus* (Grunow) Krieger, *Fragilariopsis oceanica* (Cleve) Hasle et al., *Neodenticula seminae* Simonsen and Kanaya, *Thalassionema nitzschioides* (Grunow) H. and M. Peragallo

[a]There has been considerable confusion between *Thalassiosira gravida* Cleve and *T. antarctica* var. *borealis* probably stemming from the fact that a resting spore was described and named (*Coscinodiscus subglobosus*) before either vegetative form was described [*Hasle and Syvertsen*, 1997]. This resting spore has been variously associated with either *T. gravida* [e.g., *Akiba*, 1986; *Katsuki and Takahashi*, 2005] or *T. antarctica* [e.g., *von Quillfeldt*, 2000] although *T. gravida* does not form resting spores while *T. antarctica* does [*Hasle and Syvertsen*, 1997]. In this study, all heavily silicified, coarsely areolate, convex valves with one row of marginal processes and generally several central processes were identified as *T. antarctica* resting spores. Vegetative cells of either species were rarely found.

ice-free North Pacific and perennially ice-covered Arctic Ocean. Evidence from gravity and piston cores indicates that this region has experienced fluctuations in ice extent throughout the late Pleistocene [*Sancetta and Robinson*, 1983; *Sancetta et al.*, 1985; *Nakatsuka et al.*, 1995; *Cook et al.*, 2005; *Katsuki and Takahashi*, 2005; *Okazaki et al.*, 2005]. The transition from the Last Glacial Maximum (LGM) into the Holocene was the most recent significant warming in the Arctic. Previous studies have sampled this interval in the Bering Sea every 3000 to 5000 years and have relied on qualitative associations between diatoms and sea ice [*Sancetta and Robinson*, 1983; *Sancetta et al.*, 1985; *Katsuki and Takahashi*, 2005]. Although quantitative assessments of postglacial sea ice change have been successful in other regions (e.g., North Atlantic and central Arctic basin [*de Vernal et al.*, 2005] and Antarctica [*Gersonde and Zielinski*, 2000]), circumpolar transfer functions [cf. *de Vernal et al.*, 2001] are not applicable to the Bering Sea [*Radi et al.*, 2001] and similar studies have not been attempted in the Bering Sea.

[5] Here, we build upon the growing body of western Arctic records by offering high-resolution, semiquantitative, paleoclimate data from the Umnak Plateau in the southeastern Bering Sea. We correlate relative percentages of the diatom group, *Fragilariopsis* spp., from core tops with modern sea ice conditions to show that in the Bering Sea there is an empirical relationship between *Fragilariopsis* spp. and sea ice duration. Then, we use proxy data from three types of microorganisms: diatoms, foraminifera, and coccolithophorids (Table 2) to document postglacial changes in sea ice, productivity, and SSTs. Interpretations of past sea ice and SST are based on relative changes in diatom assemblages, $\delta^{13}C$ and $\delta^{18}O$ values from planktic and benthic foraminifera, alkenone concentration, and the $U^{K'}_{37}$ temperature index. Our findings describe centennial- to millennial-scale rates of sea ice retreat that may be compared with previous longer-term diatom, geochemical, and isotope records from the North Pacific, Sea of Okhotsk, and Bering Sea [e.g., *Sancetta et al.*, 1985; *Keigwin et al.*, 1991; *Keigwin*, 1998; *Shiga and Koizumi*, 1999; *Ternois et al.*, 2000, 2001; *Sarnthein et al.*, 2001; *de Vernal et al.*, 2005; *Katsuki and Takahashi*, 2005; *Okazaki et al.*, 2005; *Sakamoto et al.*, 2005; *Sarnthein et al.*, 2006; *Gebhardt et al.*, 2008]. We find that sea ice was extensive during the LGM, covering the deep waters over Umnak Plateau. During deglaciation, the marginal ice zone extended to Umnak Plateau and sea ice had retreated north of the Umnak Plateau by 11 cal ka B.P., approximately the same time as the submergence of the Bering Strait [*Dyke et al.*, 1996; *Dyke and Savelle*, 2001; *Keigwin et al.*, 2006].

2. Background

2.1. Modern Bering Sea Physical Oceanography

[6] Today the Bering Sea is characterized by a wide, broad continental shelf 50–80 m deep in the north. Shelf waters primarily flow north through the Bering Strait to the Arctic Basin [*Schumacher and Stabeno*, 1998]. Three deeper basins: the Komandorsky, Bowers, and Aleutian basins reach depths of up to 3500 m in the south (Figure 1). Three currents constrain cyclonic circulation around the deep basins, while the Alaska Coastal Current brings 0.23 Sv of Pacific water over the shallow Unimak Pass (<80 m deep) and up onto the shelf [*Stabeno et al.*, 1999].

2.2. Sea Ice and Diatoms

[7] Today, sea ice generally forms in November over the continental shelf areas of the Bering Sea and reaches its maximum extent in March. By June, sea ice has generally retreated farther north than the Bering Strait. Ice initially forms near the Bering Strait or along the south facing coastlines and is advected southwest by the prevailing easterly winds [*Pease*, 1980; *Niebauer et al.*, 1999; *Stabeno et al.*, 1999, 2001]. When ice reaches warmer waters, it melts, slightly cooling the surface waters. In this way, ice is able to advance during the winter toward the southwest and the shelf-slope break [*Pease*, 1980; *Overland and Pease*, 1982]. The extent of sea ice is also controlled by atmospheric pressure systems. In years with a high frequency of winter cyclones, sea ice extent is reduced, because northward moving storms both physically push the ice back toward the north and at the same time bring warmer Pacific water farther north in the Bering Sea [*Overland and Pease*, 1982]. When winter sea ice is delayed in its formation, warm Pacific surface water moves into the Arctic Ocean retarding winter ice growth even further [*Serreze et al.*, 2007]. No ice is formed over the deep basins today due to the warmer water input from the Pacific [*Overland and Pease*, 1982].

[8] In years when ice extends south to the continental shelf break, there is a more intense ice-related, spring bloom because of upwelling of the higher-nutrient Bering Slope Current in the marginal ice zone [*Alexander and Niebauer*,

1981]. On the shelf, this ice-related bloom accounts for the majority of annual primary production on the Bering Sea Shelf even though it lasts only a couple of weeks [*Alexander and Niebauer*, 1981]. The ice-related bloom differs from a typical spring bloom in both locality and duration. In early spring, moderately thick (~2–4 m), clear ice transmits light so that light levels beneath the ice are well within the range for successful diatom photosynthesis. Pennate benthic species including *Fragilariopsis oceanica* and *Fragilariopsis cylindrus* attach to ice crystals at the base of the ice and take advantage of this environment [*Horner*, 1985]. The ice-related bloom continues in the water at the ice margin as the ice melts. Stratification intensifies in the water column because of the dampening effect that sea ice has on mixing and the input of fresh water due to ice melt. As dissolved silica is exhausted at the surface, the ice-related bloom sinks to the shelf bottom before all organic matter can be consumed at the surface [*Alexander and Niebauer*, 1981]. In the Bering Sea, both *F. oceanica* and *F. cylindrus* are found in the sediments and are common members of the sea ice flora [*von Quillfeldt*, 2001, and references therein] supporting the notion that diatoms found in the sediments should be robust indicators of ice extent and duration [*Alexander and Niebauer*, 1981].

2.3. Sea Surface Temperature and Alkenones

[9] Alkenones are organic biomarkers produced by a few species of coccolithophorids. The degree of alkenone unsaturation, i.e., the number of doubly bonded carbons present in these organic compounds, depends on the organism's growth temperature [*Brassell et al.*, 1986; *Herbert*, 2003; *Eglinton and Eglinton*, 2008]. *Brassell et al.* [1986] developed the alkenone unsaturation index ($U^{K'}_{37}$) to quantitatively express the degree of alkenone unsaturation: $C_{37:2}/(C_{37:2} + C_{37:3})$ where $C_{37:2}$ is the relative amount of 37-carbon diunsaturated ketones and $C_{37:3}$ is the relative amount of triunsaturated ketones. Global core top calibration studies [*Müller et al.*, 1998; *Conte et al.*, 2006] indicate the global applicability of a linear calibration function relating alkenone unsaturation index to ocean surface temperature that was originally developed by *Prahl et al.* [1988] ($U^{K'}_{37} = 0.034T + 0.039$). In higher-latitude regions, the amplitude of the seasonal cycle is much greater than at lower latitudes and coccolithophorid blooms typically occur during the summer months. Here, $U^{K'}_{37}$ temperature estimates, which are typically interpreted as reflecting mean annual SSTs, may be biased toward summer SST.

2.4. Bering Sea Since the Last Glacial Maximum

[10] Previous studies have qualitatively examined relative percent abundances of the diatom, *Fragilariopsis* spp. (previously referred to as *Nitzschia* spp.) and argued that because the eastern Bering Sea was restricted from the Pacific Ocean during the LGM (30–19 cal ka B.P.) [*Lambeck et al.*, 2002], seasonal [*Sancetta*, 1983; *Sancetta and Robinson*, 1983; *Katsuki and Takahashi*, 2005] to perennial ice was able to form [*Sancetta et al.*, 1985]. No absolute figures were proposed for what relative percentage of *Fragilariopsis* was preserved under six months or 12 months of ice. Rather, a peak in *Fragilariopsis* spp. in the sediments was assumed to indicate extensive ice coverage. This hypothesis was supported by low diatom diversity at the same time [*Sancetta et al.*, 1985]. *Nakatsuka et al.* [1995] also characterized the LGM as a time of low primary productivity based on low $\delta^{13}C$ values from planktic foraminifera. The deglaciation conversely, has been characterized as a time when sea ice retreated from the deep Bering Sea leaving it highly stratified, and highly productive with increased nutrients [*Nakatsuka et al.*, 1995; *Katsuki et al.*, 2004; *Cook et al.*, 2005; *Katsuki and Takahashi*, 2005; *Okazaki et al.*, 2005]. This is reflected by high diatom accumulation in the sediments [*Katsuki et al.*, 2004; *Katsuki and Takahashi*, 2005], positive $\delta^{15}N$ anomalies [*Nakatsuka et al.*, 1995], and peaks in $CaCO_3$ content due to large-scale coccolithophorid blooms [*Okazaki et al.*, 2005]. Green or laminated sediment layers indicating dysoxia are present throughout the Bering Sea during this interval [*Cook et al.*, 2005]. Due to low sampling resolution, very little has been published about the Holocene in the Bering Sea. *Sancetta* [1979] posits that by 8 cal ka, the modern physical oceanography had been established but does not elaborate further.

3. Methods

3.1. Sediment Cores

[11] In 2002, two sediment cores were extracted from 1466 m of water over the Umnak Plateau in the southeastern Bering Sea (54.55° N, 168.67° W). We sampled the top 560 cm of a 1956 cm long jumbo piston core, Healy 02-02 51JPC (hereafter, 51JPC), and a 22 cm long gravity multicore, Healy 02-02 50MC-c (hereafter, 50MC-c). Relative diatom assemblages were identified in 57 samples, alkenone abundances and $U^{K'}_{37}$ were measured in 26 samples and foraminiferal carbon and oxygen isotope values were determined from 137 samples.

3.2. Age Model

[12] It is likely that the upper most surface sediment was destroyed during piston coring, so the short gravity core, 50MC-c was taken at the same location in an effort to retrieve modern sediments. Magnetic susceptibility was measured every millimeter along both 50MC-c and the top 30 cm of 51JPC. The two curves were then correlated (see Figure S1).[1]

[13] The age model was constructed using a combination of ^{210}Pb dating of samples from the gravity core, 50MC-c, and ^{14}C dating of sediment from 51JPC. Because ^{210}Pb has a 22.3 year half-life, only sediment deposited within the past 100–150 years will contain unsupported ^{210}Pb [*Preiss et al.*, 1996]. Figure 2 shows a clear exponential decay downcore of both total and unsupported ^{210}Pb. The presence of unsupported ^{210}Pb confirms that the core top is modern; however, the massive, nonlaminated character of the sediments suggests significant bioturbation in the core. Because it is not appropriate to apply commonly used ^{210}Pb dating models (such as the constant rate of supply model) to bioturbated sediments [*Appleby*, 2001], we can only con-

[1] Auxiliary materials are available in the HTML. doi:10.1029/2008PA001671.

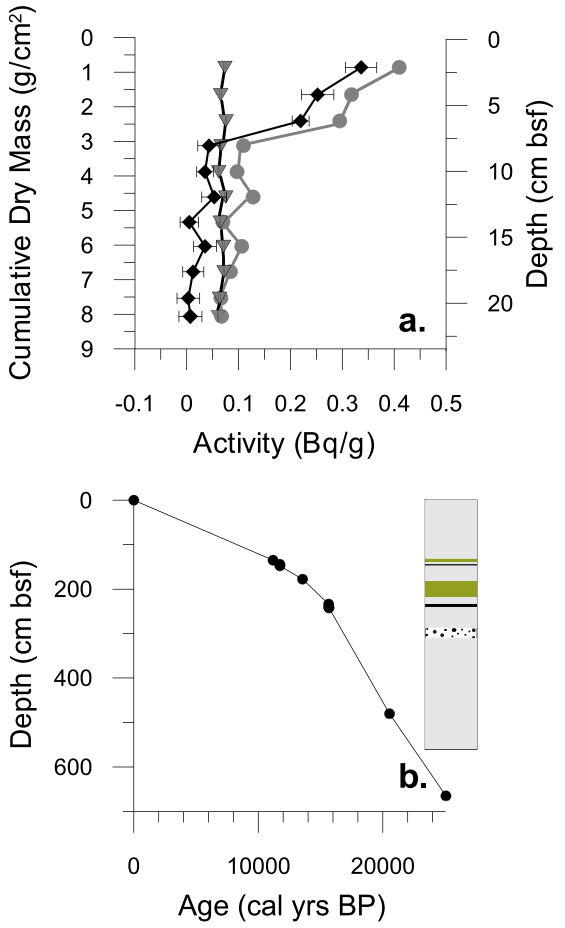

Figure 2. Combined age model for the cores 50MC-c and 51JPC. (a) Total ^{210}Pb activity (gray dots), ^{214}Pb activity (dark gray inverted triangles), and unsupported (excess) ^{210}Pb activity (black diamonds) plotted against cumulative dry mass and depth. Here ^{214}Pb is presumed in secular equilibrium with its daughter isotope, ^{210}Pb, and so is equivalent to supported ^{210}Pb. Unsupported ^{210}Pb was obtained by subtracting supported ^{210}Pb from total ^{210}Pb. (b) The age model was forced through 0 based on the presence of unsupported ^{210}Pb at the core top. Black dots deeper in the core include the five calibrated AMS ^{14}C dates measured on *N. pachyderma* (sinistral) that showed no isotopic evidence of calcite overgrowths and calculated ages for the two tephra layers [*Cook et al.*, 2005]. A reservoir age of 800 years was used throughout. All other ages are linearly interpolated between ^{14}C dates. Error bars show the standard deviation of calibrated ages and range of sediment sampled but are generally smaller than the dots. A schematic of the core is shown to the right of the plot. Gray indicates massive sediments, olive indicates laminated sediments, black indicates ash layers, and the pattern indicates the coarse interval.

clude that the core top is modern and force our age model through 0 at the top of 50MC-c.

[14] Four ^{14}C ages (Table 3) were obtained previously from the planktic foraminifera, *Neogloboquadrina pachyderma* (sinistral) [*Cook et al.*, 2005]. Because of the scarcity of foraminifera in 51JPC, we could measure only one additional ^{14}C age: the oldest at 665 cm depth. Although this is deeper than the extent of this study, this date is useful in constraining sedimentation rates during the LGM (Figure 2).

[15] A reservoir age of 800 years was used to be consistent with other published studies of these cores [e.g., *Cook et al.*, 2005; *Cook*, 2006]. However, this value is relatively poorly constrained with estimates in the region ranging from 480 to 1100 years for total modern reservoir corrections [*Kuzmin et al.*, 2001; *Dumond and Griffin*, 2002; *Kovanen and Easterbrook*, 2002]. Because the termination of the last glacial stage had pronounced impacts on thermohaline circulation [*Weaver et al.*, 2003] the reservoir age at the Umnak Plateau might have shown considerable variation during deglaciation. However, reservoir age off the coast of British Columbia, Canada appears to have remained relatively constant within 100–300 years throughout the deglaciation [*Southon and Fedje*, 2003]. We present our age model with the caveat that reservoir age may have varied by a few hundred years since the LGM.

[16] The ^{14}C ages were calibrated using Calib version 5.0.2 [*Stuiver and Reimer*, 1993] with *Hughen et al.*'s [2004] marine calibration data set. A chronology for the combined cores was modeled (Figure 2) using linear interpolation between the core top and each ^{14}C age. Two tephra layers were treated as instantaneous events. All ages are reported as calibrated calendar ages.

3.3. Sediment Processing and Analysis

3.3.1. Core Top Calibration for Relative Percent *Fragilariopsis* Versus Annual Duration of Sea Ice

[17] We examined diatom assemblage data from 134 Bering Sea core tops analyzed by *Sancetta* [1981] and made smear slides from an additional 19 core tops. Smear slides were prepared by placing 15–20 mg of sediment in distilled water, stirring, and letting it settle for approximately 10 s. A pipette was placed just above the bottom of the vial and the suspension removed. Because of this, the fines-to-coarse ratio of different samples should be comparable. Naphrax in toluene (refractive index: 1.73) was used as a mounting medium. Processing to remove the clay fraction, organic matter, or calcite was not necessary. A light microscope at magnifications of 750x to 1250x was used to identify the first 300 randomly encountered diatom valves in at least three transects across the slide following commonly accepted practice [see *Armand et al.*, 2005; *Sancetta and Silvestri*, 1986; *Sancetta*, 1979]. Partial valves were

Table 3. Radiocarbon Ages Measured on *N. pachyderma* (Sinistral)[a]

	Radiocarbon Age		Calendar Age	
Depth (cm)	^{14}C Age	1σ	Start	End
135	10,600	60	11,149	11,230
178	12,500	60	13,456	13,629
242	14,050	85	15,483	15,891
480	18,200	110	20,358	20,694
665	21,600	170	24,765	25,355

[a]Calendar ages calibrated using Calib version 5.0.2 and the Marine 04 calibration curve [*Hughen et al.*, 2004]. A total reservoir age of 800 years (ΔR = 400) was used to calculate calibrated ages [after *Cook*, 2006].

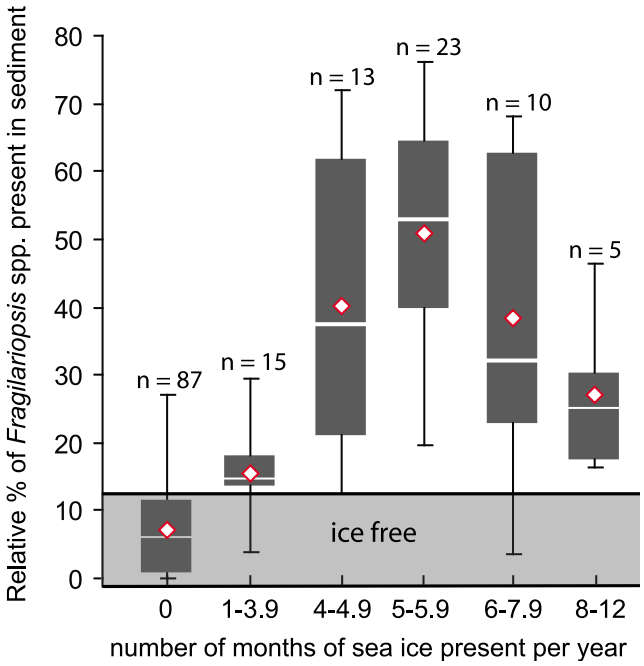

Figure 3. Box plots of relative abundance of *Fragilariopsis* spp. associated with various classes of sea ice duration. Diamonds indicate mean relative percentage of *Fragilariopsis* spp. while white bars indicate median relative percentage. Gray boxes extend to the upper and lower quartiles, while the black whiskers extend to maximum and minimum relative percentage values. The lowercase n indicates the number of samples used to construct each box plot. Sites and diatom data are from *Sancetta* [1981]. Average monthly sea ice concentrations (1978–1991) were retrieved using *Schweitzer*'s [1995] query tool, which is based on the passive microwave satellite data sets Special Sensor Microwave/Imager and scanning multichannel microwave radiometer. Annual sea ice duration is calculated according to *Crosta et al.* [1998].

counted according to the methods of *Schrader and Gersonde* [1978]. With the exception of *Fragilariopsis* spp., the pennate benthic diatoms in 51JPC were not identified to species level, nor were *Hyalochaete Chaetoceros* resting spores (hereafter referred to as *Chaetoceros* RS; all *Chaetoceros* spp. encountered are of the subgenus *Hyalochaete*). All other diatoms were identified to the species level and the counts were transformed into relative percent abundances. Diatoms were identified following the published taxonomic descriptions of *Sancetta* [1982], *Jousé* [1977], *Koizumi* [1973], and *Medlin and Priddle* [1990].

[18] The annual duration of sea ice at each core top site was derived from brightness temperatures from Special Sensor Microwave/Imager and scanning multichannel microwave radiometer passive microwave satellite data. We used a tool in the U.S. Geologic Survey's Digital Data Series [*Schweitzer*, 1995] to obtain the average monthly ice concentrations for the years 1978–1991. Monthly ice concentrations were transformed into average annual duration of ice according to the method of *Crosta et al.* [1998].

3.3.2. Diatom and Alkenone Analysis Downcore

[19] Diatom assemblage data was collected according to the process described above. Smear slides were made every 6 cm along both 50MC-c and 51JPC. We achieved a mean 400 year sampling resolution since the LGM; some sections of the core were sampled at 100 year resolution.

[20] To determine alkenone unsaturation indices and alkenone concentration, 3 cm^3 of sediment was sampled every 12 cm (mean age resolution of 700 years) along 50MC-c and 51JPC. This sediment was freeze-dried overnight and analyzed at Brown University. Alkenone concentration was measured and $U^{K'}_{37}$ temperature estimates were calculated according to procedures outlined by *Herbert and Schuffert* [1998]. Some previous work in the polar waters of the Nordic Seas has identified complications in applying the alkenone unsaturation index in cold polar regions (SST < 8°C) of Nordic Seas where concentrations of the tetraunsaturated alkenone in both water column and sediment samples are high [*Rosell-Melé*, 1998; *Bendle and Rosell-Melé*, 2004]. However, we believe these kinds of complications associated with our samples are unlikely, as the tetraunsaturated alkenone is extremely rare to absent from the Bering Sea sediment samples analyzed as part of this study.

[21] Sampling and sediment processing methods for foraminiferal isotopic work is described by *Cook et al.* [2005]. Carbon and oxygen isotopes were measured on one specimen of *Uvigerina peregrina* (benthic) and eight specimens of *Neogloboquadrina pachyderma* (sinistral; planktic) [*Cook et al.*, 2005]. The mean age resolution is approximately 300 years and duplicate or triplicate samples were run on deglacial and LGM samples when foraminiferal abundance was sufficiently high.

4. Results

4.1. Relative Percent *Fragilariopsis* spp. From Core Tops

[22] Relative percent *Fragilariopsis* spp. varies from zero to 76% in core tops from locations that experienced between zero and 11 months per year of sea ice. Box plots illustrate a normal distribution of mean and median relative percent *Fragilariopsis* spp. over annual duration of sea ice. There is a median peak of 53% *Fragilariopsis* spp. when five months of sea ice per year are present (Figure 3).

4.2. Sedimentology

[23] Both cores are composed of relatively homogenous diatomaceous dark olive green clay and silt. Two laminated intervals are present. The first occurs between 220 cm and 182 cm (15.1–13.7 cal ka B.P.) and the second between 140 cm and 132 cm (11.5–11.0 cal ka B.P.). Both laminated intervals are marked by submillimeter thick laminae ranging in color from black to dark olive green. Both are underlain by thick tephra deposits (241 cm to 234 cm and 148 cm to 144 cm) dated to 15.6 and 11.7 cal ka B.P., respectively. An interval of coarser grained sediment occurs between 310 cm and 288 cm (17.1–16.6 cal ka B.P.). There is a qualitative difference in sedimentation between the LGM and the present. Diatoms are sparse below 240 cm (15.6 cal ka B.P.) and smear slides are dominated by mineral and rock fragments in contrast to more recent sedi-

ments which are dominated by intact diatom frustules and fragments.

4.3. Diatom Record

[24] The relative percent abundances of major diatom components in 51JPC reflect oceanographic and climatologic changes over the Umnak Plateau since the LGM (Figure 4). Deeper than 222 cm (15.2 cal ka B.P.), sea ice diatoms dominate although relative percent *Fragilariopsis* spp. varies considerably between 1% and 25%. It has relative abundance values greater than 19% between 558 cm and 522 cm (22.4–21.6 cal ka B.P.) and at 438 cm (19.7 cal ka B.P.). The peak relative percent abundance of *Fragilariopsis* spp. is 41% at 198 cm (14.3 cal ka B.P.). Deeper than 222 cm, *Thalassiosira antarctica* resting spore (hereafter *T. antarctica* RS) relative percent abundance remains above 10% and at 558 cm (22.4 cal ka B.P.) it comprises 46% of the diatom assemblage. Its peak relative percent abundance of 50% occurs at 300 cm (16.9 cal ka B.P.). The relative percent abundance of pennate benthic species remains above 3% deeper than 222 cm. It has its highest values just before the first laminated interval (between 246 cm and 222 cm; 15.8–15.2 cal ka B.P.). Above 138 cm (11.3 cal ka B.P.), all three taxa are minor components of the diatom assemblage.

[25] *Thalassiosira hyalina* has a local maximum beginning at the onset of the first laminated interval (216 cm to 168 cm; 15.0–12.9 cal ka B.P.). *Thalassiosira nordenskioeldii* is virtually absent from the core until the first laminated interval (216 cm) and remains relatively high during the same intervals as *T. hyalina*. *Thalassionema nitzschioides* peaks either coeval with or immediately following *Fragilariopsis* spp. between 546 cm and 498 cm (22.1–21.0 cal ka B.P.), at 210 cm (14.7 cal ka B.P.), and between 144 cm and 138 cm (11.7–11.3). *T. nitzschioides* also has been increasing slightly since 132 cm (11.0 cal ka B.P.). *Odontella aurita* peaks during the same interval as the pennate benthic species with relative percent abundances between 28 and 37%. Its second relative abundance maximum is during the second laminated interval between 156 cm and 126 cm (12.2–10.5 cal ka B.P.).

[26] A decline of sea ice diatoms gives way to an increase in *Chaetoceros* resting spores (RS) beginning at 222 cm (15.2 cal ka B.P.) and peaking at 168 cm (12.9 cal ka B.P.) where it comprises 68% of the diatom assemblage. *Chaetoceros* RS, dominate the assemblage during the lower of two laminated sections (15.1 to 13.7 cal ka B.P.), but then by 152 cm (12 cal ka B.P.) give way to a rise in *Neodenticula seminae*. A slow transition from a *Chaetoceros* RS-dominated assemblage to an *N. seminae*–dominated assemblage occurs between 152 cm and 78 cm (12.0 cal ka B.P. and 6.5 cal ka B.P.). From 78 cm to the core top (6.5 cal ka B.P. to the present), *N. seminae* accounts for 37–51% of all diatoms found in the sediments though its relative percent abundance has been declining since 30 cm (2.5 cal ka B.P.). *Rhizosolenia hebetata* remains low (<4%) deeper than 168 cm (12.9 cal ka B.P.) and increases from 168 cm to the core top, coeval with a decline in relative percent abundance of *Chaetoceros* RS. *R. hebetata*'s highest relative percent abundance is 12% at 18 cm (1.5 cal ka B.P.).

[27] Although the relative percent abundance of *Thalassiosira trifulta* varies between 2% and 30%, it maintains a relatively constant presence of about 10% throughout. *T. trifulta* increases to near 30% of the assemblage between 486 cm and 462 cm (20.7–20.2 cal ka B.P.) and between 144 cm and 132 cm (11.7–11.0 cal ka B.P.).

[28] *Coscinodiscus marginatus*, a heavily silicified species, maintains low percent abundance throughout the core (<9%) except at 126 cm (10.5 cal ka B.P.) where it peaks at 13.8%. A high abundance of *C. marginatus* would likely indicate sediment transport, winnowing, or diatom dissolution and an assemblage that is biased toward more heavily silicified types [*Baldauf*, 1981; *Sancetta*, 1982]. The relatively constant and low abundance of this species throughout indicates that the core is probably not affected by sedimentation from afar or uneven dissolution through time.

4.4. Alkenone Record

[29] Below 294 cm (16.7 cal ka B.P.), C_{37} total alkenone concentrations were below the detection limit and remained very low (<0.16 nmol/g) until the first laminated section of the core (222 cm; 15.2 cal ka B.P.) (Figure 4). C_{37} total rises abruptly during the first laminated interval and then gradually decreases between laminated intervals. The largest peak in C_{37} total is seen when June insolation is highest in the region [*Berger and Loutre*, 1991], just after the second laminated interval at 126 cm (10.5 cal ka B.P.). After this peak, C_{37} total again gradually decreases and is low until the present. However, during the Holocene, it remains approximately 1 nmol/g higher than the minimum recorded during the LGM and early deglaciation.

[30] The $U^{K'}_{37}$ temperature index shows a quite different pattern. Before 152 cm (12.0 cal ka B.P.), $U^{K'}{}_{37}$ index indicates SSTs fluctuating between 5°C and 6°C. Temperature suddenly increases by 3°C to 8.5°C during the second laminated interval between 152 cm and 139 cm (12.0 to 11.4 cal ka B.P.) then fluctuates between 6.5°C and 8.5°C until the present. There appears to be a bias toward summertime SST as the core top $U^{K'}_{37}$ temperature estimate of 8.1°C falls close to the summer season average SST (8.5°C) [*Locarnini et al.*, 2006].

4.5. Isotope Record

[31] Between 514 cm (21.4 cal ka B.P.) and 228 cm (15.4 cal ka B.P.), $\delta^{13}C$ values in benthic foraminifera remain essentially constant at approximately −1.4 ‰. Between 228 cm and 156 cm (15.4 to 12.2 cal ka B.P.), $\delta^{13}C_{benthic}$ values increase by more than 0.5‰. After 156 cm, $\delta^{13}C_{benthic}$ values remain constant at −1.0‰. Planktic foraminiferal $\delta^{13}C$ values fluctuate widely before 228 cm (15.4 cal ka B.P.) and stabilize by 108 cm (9.0 cal ka B.P.). The gradient between benthic and planktic $\delta^{13}C$ averages 0.9‰ before 228 cm and increases to an average value of 1.4‰ in younger sediments. A lower-resolution data set of the planktic and benthic $\delta^{18}O$ values from this core was presented by *Cook et al.* [2005]. The higher-resolution data show planktic and benthic $\delta^{18}O$ values that are enriched and relatively stable earlier than 222 cm (15.2 cal ka B.P.). Benthic oxygen isotopic values decrease between 15.2 and 10.5 cal ka B.P., and are again stable throughout the Holocene. However, $\delta^{18}O_{planktic}$ suddenly becomes depleted by 1.0‰ between 222 and 216 cm (15.2 cal ka B.P. to 15.0 cal ka

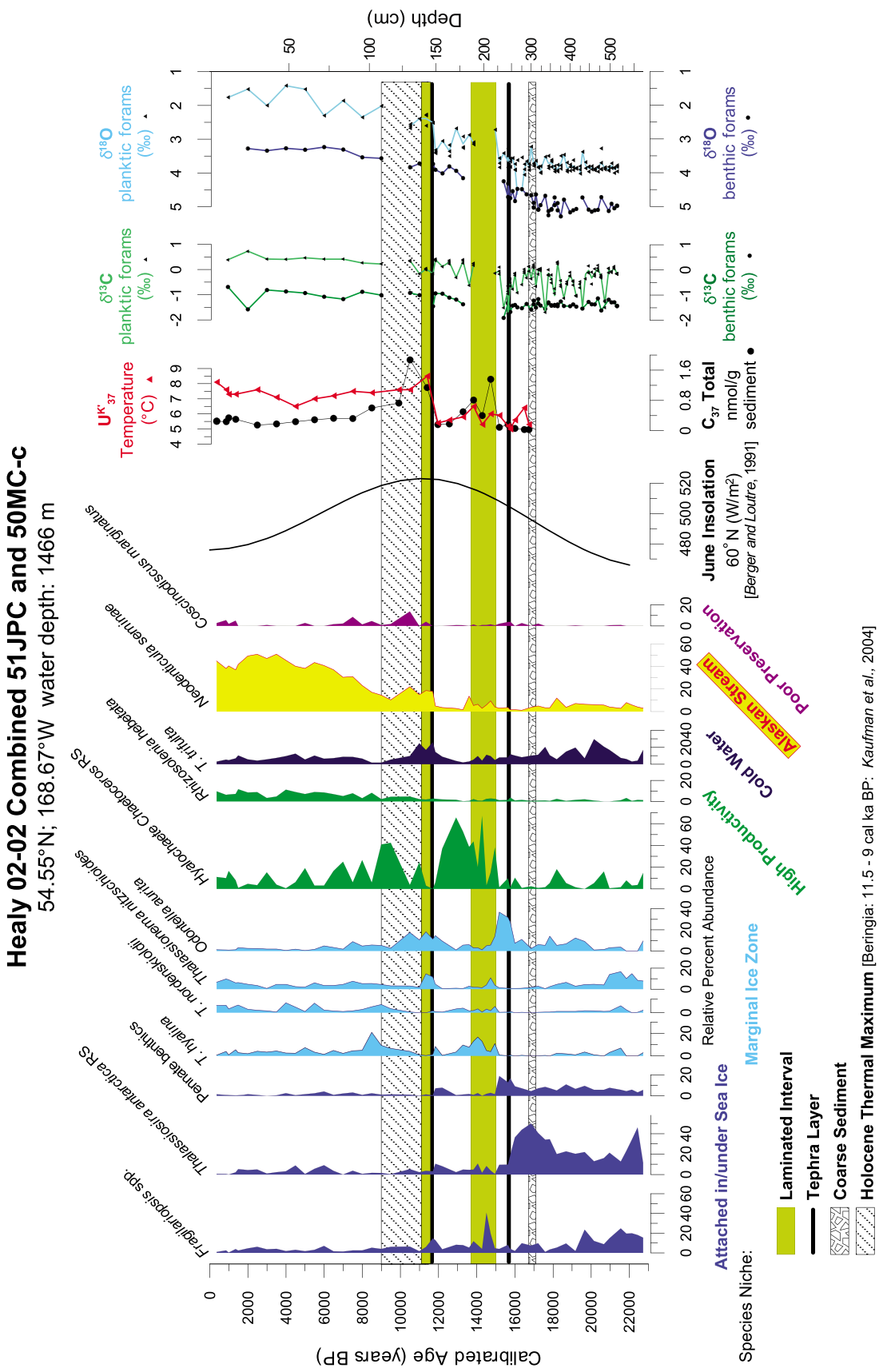
Healy 02-02 Combined 51JPC and 50MC-c
54.55°N; 168.67°W water depth: 1466 m
Depth (cm)
Calibrated Age (years BP)
Relative Percent Abundance
Species Niche:
Attached in/under Sea Ice
Marginal Ice Zone
Fragilariopsis spp.
Thalassiosira antarctica RS
Pennate benthics
T. lyvalina
T. nordenskioldii
Thalassionema nitzschioides
Odontella aurita
Hyalochaete Chaetoceros RS
Rhizosolenia hebetata
T. trifulta
Neodenticula seminae
Coscinodiscus marginatus
U^K'37 Temperature (°C)
δ13C planktic forams (‰)
δ18O planktic forams (‰)
δ13C benthic forams (‰)
δ18O benthic forams (‰)
June Insolation 60° N (W/m2) [Berger and Loutre, 1991]
C37 Total nmol/g sediment
High Productivity
Cold Water
Alaskan Stream
Poor Preservation
Laminated Interval
Tephra Layer
Coarse Sediment
Holocene Thermal Maximum [Beringia: 11.5 - 9 cal ka BP: Kaufman et al., 2004]

Figure 4

B.P.). Between 150.0 and 144.0 cm (11.8 cal ka B.P. to 11.7 cal ka B.P.) $\delta^{18}O_{planktic}$ again becomes suddenly depleted by 0.86‰. These values continue to decline to the present-day.

5. Discussion

5.1. Core Top Calibration Between *Fragilariopsis* spp. and Sea Ice Duration

[32] *Gersonde and Zielinski* [2000] argue that because diatom sediment assemblages are controlled by the composition of the spring and summer blooms rather than by the length of time ice covers an area, quantitative estimates of sea ice duration are not possible. However, diatom assemblages in core tops from the Bering Sea indicate that there is a connection between relative abundances of *Fragilariopsis* spp. and annual duration of sea ice (Figure 3) even though diatom production is low during the winter when sea ice is thick and continuous with few leads. We recognize that definitive interpretations should be made with caution when looking at only relative percent *Fragilariopsis* spp. and there is overlap between the various bins, for example, 17% *Fragilariopsis* spp. could just as likely indicate 1–4 months of sea ice annually as it could indicate 8–12 months of sea ice annually. Given these caveats, we propose the following benchmarks: (1) less than 3.5% *Fragilariopsis* spp. indicates perennially ice free times, (2) between 13% and 18% *Fragilariopsis* spp. indicates 1–4 months of sea ice per year, and (3) greater than 19% *Fragilariopsis* spp. indicates more than 4 months of sea ice per year.

[33] Certainly the ecological processes responsible for this relationship need to be investigated and this data set of core tops should be expanded to include an equal distribution of sites across all monthly bins of seasonal sea ice duration.

5.2. Last Glacial Maximum Through the Early Deglacial Period (23 ka to 17 ka): More Than 6 Months of Sea Ice Present Each Year

[34] During the LGM, the Aleutian basin was partially cut off from the North Pacific due to a lowered sea level and barriers created by glaciation of the Aleutian Islands [*Mann and Hamilton*, 1995]. This partial isolation is reflected by the low relative percentage of the Alaskan Stream indicator species: *Neodenticula seminae*, found in sediments on the Unmak Plateau of the eastern Bering Sea. Cutting the basin off from the warmer Pacific waters would have allowed perennial sea ice to develop over the deep waters of the Aleutian Basin [*Sancetta*, 1983].

[35] Several lines of evidence point to thick, extensive sea ice, possibly perennial pack ice, at Umnak Plateau prior to 17.0 cal ka B.P. An average relative percentage of 17% *Fragilariopsis* spp. between 22.7 and 19.2 ka indicate that ice was likely present over the Umnak Plateau for more than 8 months each year (Figure 4). *T. antarctica* RS, an indicator of thick pack ice [*Horner*, 1985], dominates the diatom assemblage and there are relatively high proportions of pennate benthic diatoms. All benthic diatoms found in the core must have been either living attached to the underside of sea ice [*Horner*, 1985; *von Quillfeldt et al.*, 2003] or have been transported in sea ice or currents from much shallower waters. It is more likely that the high proportions of *T. antarctica* and the pennate benthic diatoms are due to transport by ice than by currents because of the cyclonic nature of currents in the Bering Sea [*Stabeno et al.*, 1999]. Mean surface and intermediate flow over Umnak Plateau likely originated from the southwest, far from a shallow water or terrestrial source. In contrast sea ice would likely originate in coastal areas to the north and then be advected to the south/southwest by winter winds. Additionally, there are no alkenones present in the sediments during the LGM. This may be due to a lack of alkenone production or to their lack of preservation in the sediments. Alkenones degrade under oxic conditions [*Hoefs et al.*, 1998] which were likely present during the LGM as evidenced by the highly bioturbated character of the sediment. However, if alkenone degradation was the driver of low alkenone content in the sediments, we would expect alkenones to be similarly degraded during all nonlaminated intervals of the core. This is not the case. Conversely, if thick perennial sea ice was present during the LGM, coccolithophorid production would have been significantly hampered and we would expect to find few alkenones in the sediments. We propose that low coccolithophorid production resulted in little to no alkenone deposition during the LGM.

[36] While our diatom record is similar to *Sancetta and Robinson*'s [1983] Umnak Plateau record (Figure 5), our higher-resolution data set and additional alkenone record further supports *Sancetta et al.*'s [1985] hypothesis that sea ice perennially covered the area during the LGM. Diatom blooms would have been restricted to in-ice or below-ice productivity. The highly productive spring bloom that occurs around broken ice at the marginal ice zone would have occurred farther to the south or southwest than it does today. *Katsuki and Takahashi* [2005] did not find evidence for perennial ice in another Umnak Plateau core (UMK3A; Figure 5). The marked difference between relative propor-

Figure 4. Plot showing relative percent abundances of common diatom species downcore *Fragilariopsis* spp. combines both *F. cylindrus* and *F. oceanica*. RS indicates that only resting spores of that taxa are included in the plot. Diatoms are color coded according to environmental preference. Also shown is June insolation at 65°N [*Berger and Loutre*, 1991], C_{37} total alkenone concentration (black circles), U'^{K}_{37} sea surface temperature (red triangles), benthic foraminiferal $\delta^{13}C$ (black circles with dark green line), planktic foraminiferal $\delta^{13}C$ (black triangles with light green line), benthic foraminiferal $\delta^{18}O$ (black circles with dark blue line), and planktic foraminiferal $\delta^{18}O$ (black triangles with light blue line). In cases where duplicate or triplicate samples were analyzed, all values are plotted with a dot or a triangle, but the line runs through the average of the duplicates/triplicates. Isotope plots are discontinuous to show intervals of the core where foraminifera are absent. All proxies are plotted against calibrated calendar ages B.P. and depth. The Holocene thermal maximum, two laminated intervals, two ash layers, and a layer of coarse sediment are indicated behind the plot.

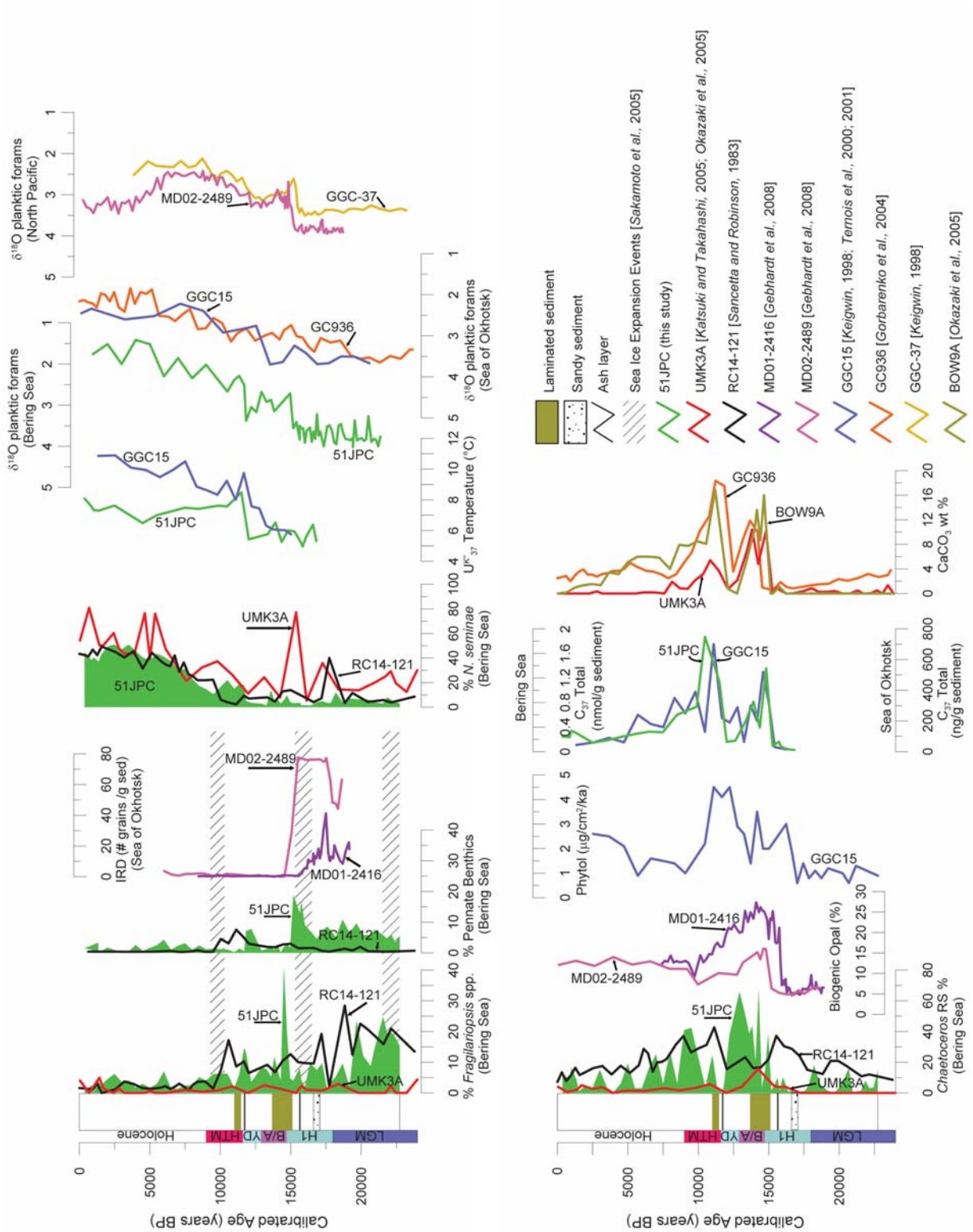
δ18O planktic forams (North Pacific)
MD02-2489
GGC-37
δ18O planktic forams (Bering Sea)
GGC15
GC936
51JPC
δ18O planktic forams (Sea of Okhotsk)
UK'37 Temperature (°C)
% N. seminae (Bering Sea)
UMK3A
RC14-121
IRD (# grains /g sed) (Sea of Okhotsk)
MD01-2416
% Pennate Benthics (Bering Sea)
% Fragilariopsis spp. (Bering Sea)
Holocene
H1
LGM
Calibrated Age (years BP)
Laminated sediment
Sandy sediment
Ash layer
Sea Ice Expansion Events [Sakamoto et al., 2005]
51JPC (this study)
UMK3A [Katsuki and Takahashi, 2005; Okazaki et al., 2005]
RC14-121 [Sancetta and Robinson, 1983]
MD01-2416 [Gebhardt et al., 2008]
MD02-2489 [Gebhardt et al., 2008]
GGC15 [Keigwin, 1998; Ternois et al., 2000; 2001]
GC936 [Gorbarenko et al., 2004]
GGC-37 [Keigwin, 1998]
BOW9A [Okazaki et al., 2005]
CaCO3 wt %
Bering Sea
C37 Total (nmol/g sediment)
Sea of Okhotsk
C37 Total (ng/g sediment)
Phytol (μg/cm2/ka)
Biogenic Opal (%)
Chaetoceros RS % (Bering Sea)

Figure 5

tions of *Fragilariopsis* spp. may be due to the slight differences in location between cores. UMK3A is slightly farther to the southwest than 51JPC; a small canyon runs between the two cores (Figure 1).

[37] Global climate models show a diverse response of sea ice to the radiative forcing and topography of the LGM, ranging from seasonal sea ice in the western Bering Sea [*Otto-Bliesner et al.*, 2006], extensive thin sea ice across the North Pacific [*Hewitt et al.*, 2003], or perennial sea ice in the Bering Sea, specifically near the Umnak Plateau [*Peltier and Solheim*, 2004].

5.3. Deglaciation From 17 ka to 10 ka: A Transition From Perennial Sea Ice to Ice-Free Conditions

5.3.1. Initial Warming

[38] At 16.9 cal ka B.P., the first indication of warming is seen after the LGM as June insolation begins to rise at 65°N [*Berger and Loutre*, 1991]. *T. antarctica* peaks coeval with the only section of the core that has a noticeably coarser grain size (Figure 4), thereby presenting the possibility that these resting spores were carried out to the Umnak Plateau by sediment-covered sea ice and deposited along with sandy sea ice rafted debris as the sea ice melted for the first time. This interval roughly corresponds with significant deposition of sea ice rafted debris in the Sea of Okhotsk from 15.3 to 16.5 cal ka B.P. [*Sakamoto et al.*, 2005] and an episode of ice rafted debris (IRD) deposited in the North Pacific between 15 and 19 cal ka B.P. [*Gebhardt et al.*, 2008]. As *T. antarctica* RS relative abundance begins to decrease, the first detectable concentration of alkenones occurs in the sediments at 16.7 cal ka B.P. (Figure 4). This is slightly earlier than the first detectable concentrations of alkenones are found in Sea of Okhotsk sediments [*Ternois et al.*, 2000, 2001]. Previous studies indicate that the total concentration of C_{37} alkenones (measured as nmol C_{37} alkenone per gram sediment) is correlated with other indices of past productivity (e.g., total organic carbon) [*Budziak et al.*, 2000; *Villanueva et al.*, 1997]. Here we use C_{37} Total, the sum of the concentration of $C_{37:2}$ and $C_{37:3}$ alkenones, as a qualitative index for paleoproductivity. Because the cosmopolitan species *Emiliani huxleyi*, by far the dominant producer of alkenones in the modern ocean, dominates in number the coccolithophorid assemblages in the Bering Sea [*Takahashi et al.*, 2002], we assume that changes in C_{37} Total are representative of significant changes in Bering Sea coccolithophorid production as a whole. We propose that deposition of alkenones in the sediments signals a change from thick pack ice over the Umnak Plateau to a more dynamic perennial ice cover. Areas of open water, polynyas, or leads near Umnak Plateau would have allowed coccolithophorids to comprise a minor part of the phytoplankton community. Although the relative percentage of *Fragilariopsis* spp. is lower than what would be expected with 8–12 months of sea ice, *T. antarctica* RS, indicators of thick pack ice, dominate the assemblage while diatom species that are characteristic of open water blooms are minor components. It is likely that ice coverage remained extensive with only short intervals of open water.

[39] *Sarnthein et al.* [2006] argue that pulses of warming in the North Pacific (up to 6°C at 18.2–17.2 ka, 16.8–16.3 ka, and 16.2–14.7 ka) created favorable conditions for early Americans migrating along the Beringian shoreline (stretching from eastern Siberia to the Yukon including the Bering and Chukchi shelves and Alaska) from Asia [*Sarnthein et al.*, 2006]. Closer to the Beringian coast, at the Umnak Plateau, we find no evidence for the first warming and are unable to quantify the second warming as alkenones are virtually absent from the sediments before 16.8 cal ka B.P. and there is little change in $\delta^{18}O$ values. However, a shift from perennial to seasonal sea ice conditions at 16.7 cal ka B.P. does indicate that the Bering Sea warmed at this time. In contrast, the North Atlantic experienced cold conditions during Heinrich Event 1 [*Sarnthein et al.*, 2001, 2006].

[40] At 15.8 cal ka B.P., a dramatic peak in *O. aurita*, a species which reflects upwelling and/or a salinity front [*Sancetta*, 1982], is the first indicator of an open-water diatom bloom. This peak represents the first step in a complete diatom assemblage turnover from an assemblage dominated by sea ice species to high-productivity species to North Pacific oceanic species.

5.3.2. Laminated Intervals

[41] One of the most striking features of 51JPC is the occurrence of submillimeter-scale laminae in periodic intervals throughout the core (15.1–13.7 cal ka B.P. and 11.5–11.0 cal ka B.P.). If these were true varves, one might expect sedimentation rates of 1–2 mm per year based on the thickness of the laminae; however, age control in this section of the core suggests sedimentation rates of less than 0.25 mm/yr, so we hypothesize that these are likely not true varves. Certainly better age control is necessary to verify this.

[42] Our data show that both laminated intervals in 51JPC are periods of increased SSTs, fresher surface waters, changes in sea ice conditions, and increased productivity. *Cook et al.* [2005] attribute the presence of these intervals to either increased surface production, suffocating the benthos as organic matter settles in thick mats, or simply increased respiration depleting oxygen from the water column. Alternatively, a change in ocean ventilation throughout the Pacific may have caused the oxygen minimum zone to expand to more than 1000 m producing laminae simultaneously in far flung regions of the North Pacific from the Santa Barbara Basin to the Sea of Japan and Bering Sea [*Cook et al.*, 2005].

Figure 5. Comparison of diatom, isotope, and coccolithophorid records from 51JPC with proxies from other cores in the Bering Sea, Sea of Okhotsk, and North Pacific. Proxies referenced in the text are plotted; additional information about their citation and location can be found in Table 1 and Figure 1. All proxy data are plotted versus calibrated calendar years B.P. Major climate events are delineated on the left, and a generalized stratigraphy of 51JPC is shown. Olive bars indicate laminated intervals, black lines indicate ash layers, and the patterned section indicates the coarser interval found in the core. Sea ice proxies are plotted above hatched bars indicating intervals of sea ice expansion in the Sea of Okhotsk [*Sakamoto et al.*, 2005].

5.3.2.1. Increased Temperature and Decreased Salinity During Laminated Intervals

[43] At the onset of each laminated interval, planktic $\delta^{18}O$ values shift by nearly 1.0‰. At ~15 cal ka B.P., a similar depletion of $\delta^{18}O$, attributed to surface freshening, warming SST, and a reduction in North Atlantic Deep Water formation, is present in cores from Bowers Ridge [*Cook et al.*, 2005], the Sea of Okhotsk [*Keigwin*, 1998], the Emperor Seamounts in the North Pacific [*Keigwin*, 1998] (Figure 5) and in cores from the Gulf of Mexico, Bermuda Rise, and Florida coast [*Keigwin et al.*, 1991].

[44] $U^{K'}_{37}$ data indicates that temperatures dramatically increased by more than 3°C at the onset of the upper laminated interval (11.5–11.0 cal ka B.P.) which corresponds with the early part of the Holocene thermal maximum (HTM) in Beringia (11.5–9 cal ka B.P.). This period of increased terrestrial and sea surface temperatures occurred several thousand years earlier here than those in eastern North America which likely warmed more slowly due to the close proximity of the Laurentide Ice Sheet [*Kaufman et al.*, 2004]. The sudden increase in SST at Umnak Plateau is likely due to a combination of two factors: as insolation rose at 60°N, the Aleutians were deglaciated, sea level rose and the far eastern sill in the Bering Sea, Unimak Pass (~50 m) was breached. Evidence for this breach can be gleaned from the increase in *N. seminae* [*Katsuki et al.*, 2004], a tracer of Pacific water (Figure 4). Increased insolation coupled with the influx of warm Pacific water led to the more than 3°C increase in $U^{K'}_{37}$ that begin at 12.0 cal ka B.P. (Figure 5). Beginning slightly earlier at 13.7 cal ka B.P., SSTs in the Sea of Okhotsk inferred from $U^{K'}_{37}$ also increased dramatically by almost 4°C (Figure 5) [*Ternois et al.*, 2000, 2001]. At the same time, a northward expansion of terrestrial ecosystems occurred in Western Alaska [*Mann and Hamilton*, 1995], and Bering Strait was flooded [*Dyke et al.*, 1996; *Dyke and Savelle*, 2001; *Keigwin et al.*, 2006; *Hill et al.*, 2007].

5.3.2.2. Changes in Sea Ice During Laminated Intervals

[45] Abrupt changes in sea ice duration occur during each laminated interval. A shift from perennial to seasonal sea ice (>4 months per year) occurs during the first laminated interval based on relatively high abundances of *T. hyalina* and *T. nordenskioeldii*, species characteristic of the marginal ice zone that bloom in succession in open waters between ice floes [*von Quillfeldt*, 2001] and relative percent *Fragilariopsis* spp. abundances of 41% (Figure 4). The high diversity of dominant species: *Fragilariopsis* spp., *T. hyalina*, *T. nordenskioeldii*, *T. nitzschioides*, *O. aurita*, *Chaetoceros* RS, *T. trifulta*, and *N. seminae* indicates that a bloom similar to the ice-related diatom bloom currently seen in the marginal ice zone on the Bering Shelf [*Taniguchi et al.*, 1976] occurred at the Umnak Plateau during this laminated interval.

[46] The diversity of diatom species during the upper laminated interval is again high, but characterized instead of by sea ice diatoms, by more cosmopolitan species like *T. nitzschioides*, the Alaska Stream indicator, *N. seminae*, a species indicative of highly stratified water with a strong temperature minimum, *T. trifulta* [*Sancetta*, 1982], and a high-productivity indicator *O. aurita* [*Sancetta*, 1982; *von Quillfeldt*, 2001; *Aizawa et al.*, 2005]. The relative abundance of sea ice diatoms decreases to near zero at the same time as temperatures peak. This suggests that at 11.3 cal ka B.P. sea ice no longer formed over the Unmak Plateau.

5.3.2.3. Increased Productivity During Laminated Intervals

[47] The high productivity of the first laminated interval is evidenced by episodic increases in relative percentages of *Chaetoceros* RS, a lightly silicified diatom genus that is one of the last to bloom [*Saitoh and Taniguchi*, 1978; *von Quillfeldt*, 2001]. The subgenus *Hyalochaete* forms small, highly ornate, heavily silicified resting spores that sink to the seafloor after essential diatom nutrients are depleted [*Round et al.*, 1990]. The spores are indicators of high productivity and upwelling because *Chaetoceros* only blooms when either nutrient levels are high enough to sustain multiple diatom blooms each year or there is a input of nutrients later in the year that allows a second diatom bloom to occur [*Abrantes*, 1988]. This increase in productivity occurs simultaneously with an increase in biogenic opal in the North Pacific [*Gebhardt et al.*, 2008] suggesting that increased diatom productivity was a widespread phenomenon during the deglacial.

[48] Paleoproductivity can be further assessed using planktic and benthic foraminiferal $\delta^{13}C$. *Uvigerina peregrina* is typically described as a shallow infaunal dweller (living at depths <1.0 cm in the sediment) [*McCorkle et al.*, 1990; *Jorissen*, 1999; *Tachikawa and Elderfield*, 2002]. *U. peregrina* tests have an isotopic value close to that of the surrounding pore waters in the sediments [*McCorkle et al.*, 1990; *Tachikawa and Elderfield*, 2002]. *N. pachyderma* (s) is a planktic species that lives in the temperature minimum zone at high latitudes [*Bauch et al.*, 2002]. This situation results in a large benthic-planktic gradient of $\delta^{13}C$. However, if upwelling of ^{13}C depleted waters drives primary productivity, then planktic foraminifera will produce tests depleted in $\delta^{13}C$ and the resulting benthic-planktic gradient of $\delta^{13}C$ would be small. During the first laminated interval, the benthic-planktic $\delta^{13}C$ gradient increases by almost 0.5‰ and remains high until the present. This may be interpreted as reflecting the higher primary productivity of postglacial surface waters.

[49] During the deglaciation, episodic increases in C_{37} total (Figure 4) correspond temporally with increases in C_{37} total in the Sea of Okhotsk [*Ternois et al.*, 2000, 2001] as well as spikes in $CaCO_3$ in both the Bering Sea [*Okazaki et al.*, 2005] and the Sea of Okhotsk [*Gorbarenko et al.*, 2004] (Figure 5) that are likely driven by coccolithophorid blooms [*Okazaki et al.*, 2005]. The first increase occurs during the first laminated interval as the Umnak Plateau transitions from perennial to seasonal ice cover. The sudden onset of several months of open water because of warming SSTs may have been enough to allow a large coccolithophorid bloom to occur for the first time since the LGM. Additionally, rising insolation serves to both warm the SSTs over the Umnak Plateau and lengthen the phytoplankton growing season. A reduction in wind speed after the LGM [*Rea*, 1994] would also have contributed to increased surface stratification and a shallower mixed layer.

[50] The most dramatic increase in C_{37} total beginning at 12.0 cal ka B.P. occurs as the Umnak Plateau transitions from being covered seasonally with sea ice to a perennially ice free region. Modeling studies indicate that coccolithophorids thrive in environments that are relatively low nutrient and highly stratified compared to diatoms which prefer turbulent conditions and pulses of nutrients [*Tozzi et al.*, 2004]. The spring breakup of sea ice provides such a nutrient pulse for diatoms today and likely did so at the Umnak Plateau before 12 cal ka B.P. The loss of this nutrient source coupled with increased stratification due to warmer surface waters may have shifted the balance from a diatom-dominated environment to a coccolithophorid-dominated environment during the HTM.

[51] The combination of high concentrations of alkenones and the presence of *Chaetoceros* RS, a high-productivity indicator, during the laminated intervals, indicates that the growing season may have been long enough and with ample nutrients to allow both diatoms and coccolithophorids to coexist in seasonal succession. However, *Chaetoceros* RS abundance fluctuates dramatically, especially during the first laminated interval, and is anticorrelated with alkenone abundance. This suggests that the relationship between diatoms and coccolithophorids in the Bering Sea is more likely one of competition and potentially reflective of the turbidity and stratification of the surface waters [e.g., *Tozzi et al.*, 2004].

5.4. Holocene From 10 ka to the Present

[52] *Sancetta* [1979] hypothesized that by 8 cal ka B.P. the Bering Sea had achieved modern oceanographic conditions. By this point in time, the Beringian shoreline had attained its approximate modern limits [from *Lambeck et al.*, 2002], all sills between the Pacific and the Bering Sea had been breached, and sea ice had not formed over the deep Aleutian Basin for several thousand years. The diatom assemblage suggests that seasonal sea ice never readvanced as far south as the Umnak Plateau during the Holocene. However, there are several changes seen in both temperature and primary productivity in the Umnak Plateau region. An increase in relative percent of *N. seminae* from 12.0 cal ka B.P. until 4.5 cal ka B.P. indicates increasing influence from Pacific waters. A similar increase in *N. seminae* is seen in other Umnak Plateau and southern continental shelf cores and is also attributed to an increase in Pacific waters [*Katsuki et al.*, 2009]. The warming based on the $U^{K'}_{37}$ index shows the same pattern as the relative abundance of *N. seminae* after 4.5 cal ka B.P. This may reflect small changes in Pacific water input through Unimak Pass. When the flow of Pacific water increased, temperatures at Umnak Plateau increased, and when it decreased, the SST values at the Umnak Plateau were influenced more by colder, Arctic waters. The decreasing trend in *Chaetoceros* RS suggests reduced diatom productivity since the HTM, although *R. hebetata*, another diatom species indicative of upwelling and high productivity increases in parallel with *N. seminae* instead of tracking the relative abundance of the high-productivity indicator *Chaetoceros* RS. The Holocene has not been marked by significant changes in temperature, productivity, or sea ice extent in the vicinity of Umnak Plateau, but neither have environmental conditions across the region been static.

6. Conclusions

[53] After the LGM, the Bering Sea experienced a warming driven by increasing high northern latitude insolation. In response to this warming, sea ice coverage at Umnak Plateau declined from thick, perennial ice to ice-free conditions in the deep, southeastern Bering Sea. This drastic shift in ecosystems is recorded in diatom assemblages, alkenone concentrations, and foraminiferal isotopic signatures derived from these sediments.

[54] Major step changes in sea ice are recorded as complete diatom assemblage turnovers. The diatom assemblage transitions from one dominated by sea ice species to one dominated by species indicative of high productivity at the onset of the first laminated interval at 15.1 cal ka B.P. We interpret this transition as a shift from perennial to seasonal sea ice coverage. The diatom assemblage again transitions from one dominated by high-productivity indicators to one dominated by open water, North Pacific species at 11.3 cal ka B.P., which we interpret as a switch from seasonal sea ice coverage to ice-free conditions.

[55] Planktic oxygen isotopic values also become enriched during these transitions reflecting warming SSTs and freshening of the surface waters. Coeval with the diatom assemblage changes and isotopic enrichment, alkenone concentrations peak reflecting high coccolithophorid production. Increased diatom and coccolithophorid productivity during the deglaciation corresponds with widespread productivity in both the North Pacific and its marginal seas [e.g., *Ternois et al.*, 2000, 2001; *Gorbarenko et al.*, 2004; *Okazaki et al.*, 2005; *Gebhardt et al.*, 2008].

[56] **Acknowledgments.** We thank John Barron (USGS) and Connie Sancetta for taxonomic assistance; Mark Leckie (UMass), Rob DeConto (UMass), Gerald Dickens, Eleanor Maddison, and one anonymous reviewer for constructive criticism of the manuscript; and Peter Schweitzer (USGS) for assistance with the Query Ice tool. We would also like to thank the officers and crew of the USCGC Healy WAGB-20 for their support during core collection. This work was supported by a grant to J.B.G. from the National Science Foundation, Office of Polar Programs Arctic Natural Sciences, and ATM Paleoclimate OPP-0002643.

References

Abrantes, F. (1988), Diatom assemblages as upwelling indicators in surface sediments off Portugal, *Mar. Geol.*, *85*, 15–39, doi:10.1016/0025-3227(88)90082-5.

Aizawa, C., M. Tanimoto, and R. W. Jordan (2005), Living diatom assemblages from North Pacific and Bering Sea surface waters during summer 1999, *Deep Sea Res., Part II*, *52*, 2186–2205, doi:10.1016/j.dsr2.2005.08.008.

Akiba, F. (1986), Middle Miocene to Quaternary diatom biostratigraphy in the Nankai Trough and Japan Trench, and modified lower Miocene through Quaternary diatom zones for middle-to-high latitudes of the North Pacific, *Initial Rep. Deep Sea Drill. Proj.*, *87*, 393–481.

Alexander, V., and H. J. Niebauer (1981), Oceanography of the eastern Bering Sea ice-edge

zone in spring, *Limnol. Oceanogr.*, *26*(6), 1111–1125.

Appleby, P. (2001), Chronostratigraphic techniques in recent sediments in *Tracking Environmental Change Using Lake Sediments*, vol. 1, edited by W. M. Last and J. P. Smol, pp. 171–203, Kluwer Acad., Dordrecht, Netherlands.

Armand, L. K., X. Crosta, O. Romero, and J. J. Pichon (2005), The biogeography of major diatom taxa in Southern Ocean sediments: 1. Sea ice related species, *Palaeogeogr. Palaeoclimatol. Palaeoecol.*, *223*, 93–126, doi:10.1016/j.palaeo.2005.02.015.

Arzel, O., T. Fichefet, and H. Goosse (2006), Sea ice evolution over the 20th and 21st centuries as simulated by current AOGCMs, *Ocean Modell.*, *12*, 401–415, doi:10.1016/j.ocemod.2005.08.002.

Baldauf, J. G. (1981), Diatoms from Late Quaternary sediments from the Navarin Basin Province, in *Seafloor Geologic Hazards, Sedimentology, and Bathymetry: Navarin Basin Province, Northwestern Bering Sea*, edited by P. R. Carlson, *U.S. Geol. Surv. Open File Rep.*, *81–1217*, 100–113.

Bauch, D., H. Erlenkeuser, G. Winckler, G. Pavlova, and J. Thiede (2002), Carbon isotopes and habitat of polar planktic foraminifera in the Okhotsk Sea: The "carbonate ion effect" under natural conditions, *Mar. Micropaleontol.*, *45*, 83–99.

Bendle, J., and A. Rosell-Melé (2004), Distributions of U^{37}_K and $U^{37'}_K$ in the surface waters and sediments of the Nordic Seas: Implications for paleoceanography, *Geochem. Geophys. Geosyst.*, *5*, Q11013, doi:10.1029/2004GC000741.

Berger, A., and M. F. Loutre (1991), Insolation values for the climate of the last 10 million years, *Quat. Sci. Rev.*, *10*, 297–317.

Brassell, S. C., G. Eglinton, I. T. Marlowe, U. Pflaumann, and M. Sarnthein (1986), Molecular stratigraphy: A new tool for climatic assessment, *Nature*, *320*, 129–133, doi:10.1038/320129a0.

Budziak, D., R. R. Schneider, F. Rostek, P. J. Müller, E. Bard, and G. Wefer (2000), Late Quaternary insolation forcing on total organic carbon and C_{37} alkenone variations in the Arabian Sea, *Paleoceanography*, *15*, 307–321, doi:10.1029/1999PA000433.

CLIMAP Project Members (1981), Seasonal reconstructions of the Earth's surface at the Last Glacial Maximum, *Map Chart Ser. MC-36*, Geol. Soc. of Am., Boulder, Colo.

Conte, M. H., M.-A. Sicre, C. Rühlemann, J. C. Weber, S. Schulte, D. Schulz-Bull, and T. Blanz (2006), Global temperature calibration of the alkenone unsaturation index ($U^{K'}_{37}$) in surface waters and comparison with surface sediments, *Geochem. Geophys. Geosyst.*, *7*, Q02005, doi:10.1029/2005GC001054.

Cook, M. S. (2006), The paleoceanography of the Bering Sea during the last glacial cycle, Ph.D. dissertation, Mass. Inst. of Technol., Cambridge.

Cook, M. S., L. D. Keigwin, and C. A. Sancetta (2005), The deglacial history of surface and intermediate water of the Bering Sea, *Deep Sea Res., Part II*, *52*, 2163–2173, doi:10.1016/j.dsr2.2005.07.004.

Crosta, X., J.-J. Pinchon, and L. H. Burckle (1998), Application of modern analog technique to marine Antarctic diatoms: Reconstruction of maximum sea-ice extent at the Last Glacial Maximum, *Paleoceanography*, *13*, 284–297, doi:10.1029/98PA00339.

de Vernal, A., et al. (2001), Dinoflagellate cyst assemblages as tracers of sea-surface conditions in the northern North Atlantic, Arctic and sub-Arctic seas: The new "*n* = 677" data base and its application for quantitative palaeoceanographic reconstruction, *J. Quat. Sci.*, *16*, 681–698, doi:10.1002/jqs.659.

de Vernal, A., C. Hillaire-Marcel, and D. A. Darby (2005), Variability of sea ice cover in the Chukchi Sea (western Arctic Ocean) during the Holocene, *Paleoceanography*, *20*, PA4018, doi:10.1029/2005PA001157.

Dumond, D. E., and D. G. Griffin (2002), Measurements of the marine reservoir effect on radiocarbon ages in the eastern Bering Sea, *Arctic*, *55*, 77–86.

Dyke, A. S., and J. M. Savelle (2001), Holocene history of the Bering Sea bowhead whale (*Balaena mysticetus*) in its Beaufort Sea summer grounds off southwestern Victoria Island, western Canadian Arctic, *Quat. Res.*, *55*, 371–379, doi:10.1006/qres.2001.2228.

Dyke, A. S., J. E. Dale, and R. N. McNeely (1996), Marine molluscs as indicators of environmental change in glaciated North America and Greenland during the last 18 000 years, *Geogr. Phys. Quat.*, *50*(2), 125–184.

Eglinton, T. I., and G. Eglinton (2008), Molecular proxies for paleoclimatology, *Earth Planet. Sci. Lett.*, *275*, 1–16, doi:10.1016/j.epsl.2008.07.012.

Gebhardt, H., M. Sarnthein, P. M. Grootes, T. Kiefer, H. Kuehn, F. Schnieder, and U. Röhl (2008), Paleonutrient and productivity records from the subarctic North Pacific for Pleistocene glacial terminations I to V, *Paleoceanography*, *23*, PA4212, doi:10.1029/2007PA001513.

Gersonde, R., and U. Zielinski (2000), The reconstruction of Late Quaternary Antarctic sea-ice distribution—The use of diatoms as a proxy for sea-ice, *Palaeogeogr. Palaeoclimatol. Palaeoecol.*, *162*, 263–286, doi:10.1016/S0031-0182(00)00131-0.

Gorbarenko, S. A., J. R. Southon, L. D. Keigwin, M. V. Cherepanova, and I. G. Gvozdeva (2004), Late Pleistocene–Holocene oceanographic variability in the Okhotsk Sea: Geochemical, lithological and paleontological evidence, *Palaeogeogr. Palaeoclimatol. Palaeoecol.*, *209*, 281–301, doi:10.1016/j.palaeo.2004.02.013.

Hasle, G. R., and E. E. Syvertsen (1997), Marine diatoms, in *Identifying Marine Phytoplankton*, edited by C. R. Tomas, pp. 5–385, Academic, San Diego, Calif.

Herbert, T. D. (2003), Alkenone paleotemperature determinations, in *Treatise on Marine Geochemistry*, edited by H. Elderfield, pp. 391–432, Elsevier, Amsterdam.

Herbert, T. D., and J. D. Schuffert (1998), Alkenone unsaturation estimates of late Miocene through late Pliocene sea-surface temperatures at Site 958, *Proc. Ocean Drill. Program Sci. Results*, *159T*, 17–21.

Hewitt, C. D., C. A. Senior, and J. F. B. Mitchell (2001), The impact of dynamic sea-ice on the climatology and climate sensitivity of a GCM: A study of past, present, and future climates, *Clim. Dyn.*, *17*, 655–668, doi:10.1007/s003820000140.

Hewitt, C. D., R. J. Stouffer, A. J. Broccoli, J. F. B. Mitchell, and P. J. Valdes (2003), The effect of ocean dynamics in a coupled GCM simulation of the Last Glacial Maximum, *Clim. Dyn.*, *20*, 203–218.

Hill, J. C., N. W. Driscoll, J. Brigham-Grette, J. P. Donnelly, P. T. Gayes, and L. Keigwin (2007), New evidence for high discharge to the Chukchi shelf since the Last Glacial Maximum, *Quat. Res.*, *68*, 271–279, doi:10.1016/j.yqres.2007.04.004.

Hoefs, M. J. L., G. J. M. Versteegh, W. I. C. Rijpstra, J. W. de Leeuw, and J. S. Sinninghe Damsté (1998), Postdepositional oxic degradation of alkenones: Implications for the measurement of palaeo sea surface temperatures, *Paleoceanography*, *13*, 42–49, doi:10.1029/97PA02893.

Holland, M. M., C. M. Bitz, and B. Tremblay (2006), Future abrupt reductions in the summer Arctic sea ice, *Geophys. Res. Lett.*, *33*, L23503, doi:10.1029/2006GL028024.

Horner, R. A. (Ed.) (1985), *Sea-Ice Biota*, 215 pp., CRC Press, Boca Raton, Fla.

Hughen, K. A., et al. (2004), Marine04 marine radiocarbon age calibration, 0–26 cal kyr BP, *Radiocarbon*, *46*, 1059–1086.

Intergovernmental Panel on Climate Change (2007), *Climate Change 2007: The Physical Science Basis: Working Group I Contribution to the Fourth Assessment Report of the IPCC*, edited by S. Solomon et al., Cambridge Univ. Press, New York.

International Study of Arctic Change (2009), The International Study of Arctic Change, science plan and implementation, strategy, Int. Study of Arctic Change Program Off., Stockholm, in press.

Jorissen, F. J. (1999), Benthic foraminiferal microhabitats below the sediment-water interface, in *Modern Foraminifera*, edited by B. K. Sen Gupta, pp. 161–179, Kluwer Acad., Boston, Mass.

Jousé, A. P. (1977), *Atlas of Microorganisms in Bottom Sediments of the Oceans (Diatoms, Radiolaria, Silicoflagellates and Coccoliths)*, Nauka, Moscow.

Katsuki, K., and K. Takahashi (2005), Diatoms as paleoenvironmental proxies for seasonal productivity, sea-ice and surface circulation in the Bering Sea during the Late Quaternary, *Deep Sea Res., Part II*, *52*, 2110–2130, doi:10.1016/j.dsr2.2005.07.001.

Katsuki, K., K. Takahashi, and K. Matsushita (2004), Diatom paleoceanography during the past 340 kyr in the Bering Sea and the western subarctic Pacific, in *Seventeenth International Diatom Symposium*, edited by M. Poulin, pp. 147–159, Biopress, Bristol, U. K.

Katsuki, K., B.-K. Khim, T. Itaki, N. Harada, H. Sakai, T. Ikeda, K. Takahashi, Y. Okazaki, and H. Asahi (2009), Land-sea linkage of Holocene paleoclimate on the southern Bering Continental Shelf, *Holocene*, *19*(5), 747–756, doi:10.1177/0959683609105298.

Kaufman, D. S., et al. (2004), Holocene thermal maximum in the western Arctic (0–180°W), *Quat. Sci. Rev.*, *23*, 529–560, doi:10.1016/j.quascirev.2003.09.007.

Keigwin, L. D. (1998), Glacial-age hydrography of the far northwest Pacific Ocean, *Paleoceanography*, *13*, 323–339, doi:10.1029/98PA00874.

Keigwin, L. D., G. A. Jones, S. J. Lehman, and E. A. Boyle (1991), Deglacial meltwater discharge, North Atlantic deep circulation, and abrupt climate change, *J. Geophys. Res.*, *96*, 16,811–16,826, doi:10.1029/91JC01624.

Keigwin, L. D., J. P. Donnelly, M. S. Cook, N. W. Driscoll, and J. Brigham-Grette (2006), Rapid sea-level rise and Holocene climate in the Chukchi Sea, *Geology*, *34*(10), 861–864, doi:10.1130/G22712.1.

Kim, S.-J., T. J. Crowley, D. J. Erickson, B. Govindasamy, P. B. Duffy, and B. Y. Lee (2008), High-resolution climate simulation of the Last Glacial Maximum, *Clim. Dyn.*, *31*, 1–16, doi:10.1007/s00382-007-0332-z.

Koizumi, I. (1973), The Late Cenozoic diatoms of Sites 183–193, Leg 19 Deep Sea Drilling Project, *Initial Rep. Deep Sea Drill. Proj.*, *19*, 805–855.

Kovanen, D. J., and D. J. Easterbrook (2002), Paleodeviations of radiocarbon marine reservoir values for the northeast Pacific, *Geology*, *30*(3), 243–246, doi:10.1130/0091-7613(2002)030<0243:PORMRV>2.0.CO;2.

Kuzmin, Y. V., G. S. Burr, and A. J. T. Jull (2001), Radiocarbon reservoir correlation ages in the Peter the Great Gulf, Sea of Japan, and eastern coast of the Kunashir, southern Kuriles (northwestern Pacific), *Radiocarbon*, *43*, 477–481.

Lambeck, K., Y. Yokoyama, and T. Purcell (2002), Into and out of the Last Glacial Maximum: Sea-level changes during oxygen isotope stages 3 and 2, *Quat. Sci. Rev.*, *21*, 343–360, doi:10.1016/S0277-3791(01)00071-3.

Locarnini, R. A., A. V. Mishonov, J. I. Antonov, T. P. Boyer, and H. E. Garcia (2006), *World Ocean Atlas 2005*, vol. 1, *Temperature*, *NOAA Atlas NESDIS*, vol. 61, edited by S. Levitus, 182 pp., NOAA, Silver Spring, Md.

Lovvorn, J. R., L. W. Cooper, M. L. Brooks, C. C. De Ruyck, J. K. Bump, and J. M. Grebmeier (2005), Organic matter pathways to zooplankton and benthos under pack ice in late winter and open water in late summer in the north-central Bering Sea, *Mar. Ecol. Prog. Ser.*, *291*, 135–150, doi:10.3354/meps291135.

Mann, D. H., and T. D. Hamilton (1995), Late Pleistocene and Holocene paleoenvironments of the North Pacific coast, *Quat. Sci. Rev.*, *14*, 449–471, doi:10.1016/0277-3791(95)00016-I.

Masson-Delmotte, V., et al. (2006), Past and future polar amplification of climate change: Climate model intercomparisons and ice-core constraints, *Clim. Dyn.*, *26*, 513–529, doi:10.1007/s00382-005-0081-9.

McCorkle, D. C., L. D. Keigwin, B. H. Corliss, and S. R. Emerson (1990), The influence of microhabitats on the carbon isotopic composition of deep-sea benthic foraminifera, *Paleoceanography*, *5*, 161–185, doi:10.1029/PA005i002p00161.

Medlin, L. K., and J. Priddle (1990), *Polar Marine Diatoms*, Br. Antarct. Surv., Nat. Environ. Res. Counc., Cambridge, U. K.

Müller, P. J., G. Kirst, G. Ruhland, I. von Storch, and A. Rosell-Melé (1998), Calibration of the alkenone paleotemperature index $U^{K'}_{37}$ on core-tops from the eastern South Atlantic and the global ocean (60°N–60°S), *Geochim. Cosmochim. Acta*, *62*, 1757–1772, doi:10.1016/S0016-7037(98)00097-0.

Nakatsuka, T., K. Watanabe, N. Handa, E. Matsumoto, and E. Wada (1995), Glacial to interglacial surface nutrient variations of Bering deep basins recorded by $\delta^{13}C$ and $\delta^{15}N$ of sedimentary organic matter, *Paleoceanography*, *10*, 1047–1061, doi:10.1029/95PA02644.

Niebauer, H. J., N. A. Bond, L. P. Yakunin, and V. V. Plotnikov (1999), An update on the climatology and sea ice of the Bering Sea, in *Dynamics of the Bering Sea*, edited by T. R. Loughlin and K. Ohtani, pp. 22–59, Univ. of Alaska Sea Grant, Fairbanks.

Okazaki, Y., K. Takahashi, H. Asahi, K. Katsuki, J. Hori, H. Yasuda, Y. Sagawa, and H. Tokuyama (2005), Productivity changes in the Bering Sea during the Late Quaternary, *Deep Sea Res., Part II*, *52*, 2150–2162, doi:10.1016/j.dsr2.2005.07.003.

Otto-Bliesner, B. L., E. C. Brady, G. Clauzet, R. Tomas, S. Levis, and Z. Kothavala (2006), Last Glacial Maximum and Holocene climate in CCSM3, *J. Clim.*, *19*, 2526–2544, doi:10.1175/JCLI3748.1.

Overland, J. E., and C. H. Pease (1982), Cyclone climatology of the Bering Sea and its relation to sea ice extent, *Mon. Weather Rev.*, *110*, 5–13, doi:10.1175/1520-0493(1982)110<0005:CCOTBS>2.0.CO;2.

Pease, C. H. (1980), Eastern Bering Sea ice processes, *Mon. Weather Rev.*, *108*, 2015–2023, doi:10.1175/1520-0493(1980)108<2015:EBSIP>2.0.CO;2.

Peltier, W. R., and L. P. Solheim (2004), The climate of the Earth at Last Glacial Maximum: Statistical equilibrium state and a mode of internal variability, *Quat. Sci. Rev.*, *23*, 335–357, doi:10.1016/j.quascirev.2003.07.003.

Prahl, F. G., L. A. Muehlhausen, and D. L. Zahnle (1988), Further evaluation of long-chain alkenones as indicators of paleoceanographic conditions, *Geochim. Cosmochim. Acta*, *52*, 2303–2310, doi:10.1016/0016-7037(88)90132-9.

Preiss, N., M.-A. Mélières, and M. Pourchet (1996), A compilation of data on lead 210 concentration in surface air and fluxes at the air-surface and water-sediment interfaces, *J. Geophys. Res.*, *101*, 28,847–28,862, doi:10.1029/96JD01836y6.

Radi, T., A. de Vernal, and O. Peyron (2001), Relationships between dinoflagellate cyst assemblages in surface sediment and hydrographic conditions in the Bering and Chukchi seas, *J. Quat. Sci.*, *16*, 667–680, doi:10.1002/jqs.652.

Rea, D. K. (1994), The paleoclimatic record provided by eolian deposition in the deep sea: The geologic history of wind, *Rev. Geophys.*, *32*(2), 159–195, doi:10.1029/93RG03257.

Rosell-Melé, A. (1998), Interhemispheric appraisal of the value of alkenone indices as temperature and salinity proxies in high-latitude locations, *Paleoceanography*, *13*, 694–703, doi:10.1029/98PA02355.

Round, F. E., R. M. Crawford, and D. G. Mann (1990), *The Diatoms: Biology and Morphology of the Genera*, 747 pp., Cambridge Univ. Press, Cambridge, U. K.

Saitoh, K., and A. Taniguchi (1978), Phytoplankton communities in the Bering Sea and adjacent seas II: Spring and summer communities in seasonally ice-covered areas, *Astarte*, *11*(1), 27–35.

Sakamoto, T., M. Ikehara, K. Aoki, K. Iijima, T. Nakatsuka, and M. Wakatsuchi (2005), Ice-rafted debris (IRD)-based sea-ice expansion events during the past 100 kyrs in the Okhotsk Sea, *Deep Sea Res., Part II*, *52*, 2275–2301, doi:10.1016/j.dsr2.2005.08.007.

Sancetta, C. (1979), Use of semiquantitative microfossil data for paleoceanography, *Geology*, *7*(2), 88–92, doi:10.1130/0091-7613(1979)7<88:UOSMDF>2.0.CO;2.

Sancetta, C. (1981), Oceanographic and ecologic significance of diatoms in surface sediments of the Bering and Okhotsk seas, *Deep Sea Res., Part A*, *28*, 789–817.

Sancetta, C. (1982), Distribution of diatom species in surface sediments of the Bering and Okhotsk seas, *Micropaleontology*, *28*, 221–257, doi:10.2307/1485181.

Sancetta, C. (1983), Effect of Pleistocene glaciation upon oceanographic characteristics of the North Pacific Ocean and Bering Sea, *Deep Sea Res., Part A*, *30*, 851–869, doi:10.1016/0198-0149(83)90004-3.

Sancetta, C., and S. W. Robinson (1983), Diatom evidence on Wisconsin and Holocene events in the Bering Sea, *Quat. Res.*, *20*, 232–245, doi:10.1016/0033-5894(83)90079-0.

Sancetta, C., and S. Silvestri (1986), Pliocene-Pleistocene evolution of the North Pacific Ocean-atmosphere system, interpreted from fossil diatoms, *Paleoceanography*, *1*, 163–180, doi:10.1029/PA001i002p00163.

Sancetta, C., L. Heusser, L. Labeyrie, A. S. Naidu, and S. W. Robinson (1985), Wisconsin—Holocene paleoenvironment of the Bering Sea: Evidence from diatoms, pollen, oxygen isotopes and clay minerals, *Mar. Geol.*, *62*, 55–68, doi:10.1016/0025-3227(84)90054-9.

Sarnthein, M., et al. (2001), Fundamental modes and abrupt changes in North Atlantic circulation and climate over the last 60 ky: Concepts, reconstruction and numerical modeling, in *The Northern North Atlantic: A Changing Environment*, edited by P. Schäfer et al., pp. 365–410, Springer, Berlin.

Sarnthein, M., T. Kiefer, P. M. Grootes, H. Elderfield, and H. Erlenkeuser (2006), Warmings in the far northwestern Pacific promoted pre-Clovis immigration to America during Heinrich event 1, *Geology*, *34*(3), 141–144, doi:10.1130/G22200.1.

Schrader, H. J., and R. Gersonde (1978), Diatoms and silicoflagellates, in *Micropaleontological Counting Methods and Techniques: An Exercise on an Eight Metres Section of the Lower Pliocene of Capo Rossello, Sicily*, *Utrecht Micropaleontol. Bull.*, vol. 17, edited by W. J. Zachariasse et al., pp. 129–176, Utrecht, Schotanus and Jens, Odijk, Netherlands.

Schumacher, J. D., and P. J. Stabeno (1998), Continental shelf of the Bering Sea, in *The Sea*, vol. 11, *The Global Coastal Ocean: Regional Studies and Synthesis*, edited by A. R. Robinson and K. H. Brink, pp. 789–822, John Wiley, New York.

Schweitzer, P. N. (1995), Monthly average polar sea-ice concentration, *U.S. Geol. Surv. Digital Data Ser., DDS-27*.

Serreze, M., M. M. Holland, and J. Stroeve (2007), Perspectives on the Arctic's shrinking sea-ice cover, *Science*, *315*, 1533–1536.

Shiga, K., and I. Koizumi (1999), Latest Quaternary oceanographic changes in the Okhotsk Sea based on diatom records, *Mar. Micropaleontol.*, *38*, 91–117, doi:10.1016/S0377-8398(99)00041-9.

Southon, J., and D. Fedje (2003), A post-glacial record of ^{14}C reservoir ages for the British Columbia coast, *Can. J. Archaeol.*, *27*, 95–111.

Stabeno, P. J., J. D. Schumacher, and K. Ohtani (1999), The physical oceanography of the Bering Sea, in *Dynamics of the Bering Sea: A Summary of Physical, Chemical, and Biological Characteristics, and a Synopsis of Research on the Bering Sea*, edited by T. R. Loughlin and K. Ohtani, *Alaska Sea Grant College Program Rep. AK-SG-99-03*, pp. 1–28, Univ. of Alaska Sea Grant, Fairbanks.

Stabeno, P. J., N. A. Bond, N. B. Kachel, S. A. Salo, and J. D. Schumacher (2001), On the temporal variability of the physical environment over the south-eastern Bering Sea, *Fish. Oceanogr.*, *10*(1), 81–98, doi:10.1046/j.1365-2419.2001.00157.x.

Stockwell, D. A., T .E. Whitledge, S. I. Zeeman, K. O. Coyle, J. M. Napp, R. D. Brodeur, A. I. Pinchuk, and G. L. Hunt Jr. (2001), Anomalous conditions in the south-eastern Bering Sea, 1997: Nutrients, phytoplankton and zooplankton, *Fish. Oceanogr.*, *10*(1), 99–116, doi:10.1046/j.1365-2419.2001.00158.x.

Stroeve, J., and W. Meier (1999), Sea Ice Trends and Climatologies from SMMR and SSM/I, June to September 2001, http://nsidc.org/data/nsidc-0192.html, Natl. Snow and Ice Data Cent., Boulder, Colo.

Stroeve, J., M. Serreze, S. Drobot, S. Gearheard, M. Holland, J. Maslanik, W. Meier, and T. Scambos (2008), Arctic sea ice extent plummets in 2007, *Eos Trans. AGU*, *89*, doi:10.1029/2008EO020001.

Study of Environmental Arctic Change (2005), Study of environmental Arctic change: Plans for implementation during the international polar year and beyond, 104 pp., Antarct. Res. Consortium of the U.S., Fairbanks, Alaska.

Stuiver, M., and P. J. Reimer (1993), Extended ^{14}C database and revised CALIB radiocarbon calibration program, *Radiocarbon*, *35*, 215–230.

Tachikawa, K., and H. Elderfield (2002), Microhabitat effects on Cd/Ca and δ^{13}C of benthic foraminifera, *Earth Planet. Sci. Lett.*, *202*, 607–624, doi:10.1016/S0012-821X(02)00796-3.

Takahashi, K., N. Fujitani, and M. Yanada (2002), Long term monitoring of particle fluxes in the Bering Sea and the central subarctic Pacific Ocean, 1990–2000, *Prog. Oceanogr.*, *55*, 95–112, doi:10.1016/S0079-6611(02)00072-1.

Taniguchi, A., K. Saito, A. Koyama, and M. Fukuchi (1976), Phytoplankton communities in the Bering Sea and Adjacent Seas: I. Communities in early warming season in southern areas, *J. Oceanogr. Soc. Jpn.*, *32*, 99–106, doi:10.1007/BF02107038.

Ternois, Y., K. Kawaura, N. Ohkouchi, and L. Keigwin (2000), Alkenone sea surface temperature in the Okhotsk Sea for the last 15 kyr, *Geochem. J.*, *34*, 283–293.

Ternois, Y., K. Kawamura, L. Keigwin, N. Ohkouchi, and T. Nakatsuka (2001), A biomarker approach for assessing marine and terrigenous inputs to the sediments of Sea of Okhotsk for the last 27,000 years, *Geochim. Cosmochim. Acta*, *65*, 791–802.

Tozzi, S., O. Schofield, and P. Falkowski (2004), Historical climate change and ocean turbulence as selective agents for two key phytoplankton functional groups, *Mar. Ecol. Prog. Ser.*, *274*, 123–132, doi:10.3354/meps274123.

Villanueva, J., J. O. Grimalt, E. Cortijo, L. Vidal, and L. Labeyrie (1997), A biomarker approach to the organic matter deposited in the North Atlantic during the last climatic cycle, *Geochim. Cosmochim. Acta*, *61*, 4633–4646, doi:10.1016/S0016-7037(97)83123-7.

von Quillfeldt, C. H. (2000), Common diatom species in Arctic spring blooms: Their distribution and abundance, *Bot. Mar.*, *43*, 499–516.

von Quillfeldt, C. H. (2001), Identification of some easily confused common diatom species in Arctic spring blooms, *Bot. Mar.*, *44*, 375–389, doi:10.1515/BOT.2001.048.

von Quillfeldt, C. H., W. G. Ambrose Jr., and L. M. Clough (2003), High number of diatom species in first-year ice from the Chukchi Sea, *Polar Biol.*, *26*, 806–818, doi:10.1007/s00300-003-0549-1.

Walsh, J. J., and C. P. McRoy (1986), Ecosystem analysis in the southeastern Bering Sea, *Cont. Shelf Res.*, *5*, 259–288, doi:10.1016/0278-4343(86)90018-X.

Wang, M., and J. E. Overland (2009), A sea ice free summer Arctic within 30 years?, *Geophys. Res. Lett.*, *36*, L07502, doi:10.1029/2009GL037820.

Weaver, A. J., O. A. Saenko, P. U. Clark, and J. X. Mitrovica (2003), Meltwater pulse 1A from Antarctica as a trigger of the Bølling-Allerød warm interval, *Science*, *299*, 1709–1713, doi:10.1126/science.1081002.

J. Brigham-Grette and B. E. Caissie, Department of Geosciences, University of Massachusetts Amherst, 233 Morrill Science Center, 611 N. Pleasant St., Amherst, MA 01301, USA. (bethc@geo.umass.edu)

M. S. Cook, Geosciences Department, Williams College, 947 Main St., Williamstown, MA 01267, USA.

T. D. Herbert, Department of Geological Sciences, Brown University, 324 Brook St., Box 1846, Providence, RI 02912, USA.

K. T. Lawrence, Department of Geology and Environmental Geosciences, Lafayette College, 102 Van Wickle Hall, Easton, PA 18042, USA.